NAVAL POSTGRADUATE SCHOOL

Monterey, California

THESIS

EVALUATION OF RADAR PERFORMANCE
DEGRADATION
DUE TO STANDOFF JAMMING

by

CHI, YOON KYU

September, 1992

Thesis Advisor: G.S. Gill

Approved for public release; distribution is unlimited

UNCLASSIFIED

SECURITY CLASSIFICATION OF THIS PAGE

REPORT DOCUMENTATION PAGE

1a REPORT SECURITY CLASSIFICATION: UNCLASSIFIED	1b RESTRICTIVE MARKINGS
2a SECURITY CLASSIFICATION AUTHORITY	3 DISTRIBUTION/AVAILABILITY OF REPORT: Approved for public release: Distribution is unlimited
2b DECLASSIFICATION/DOWNGRADING SCHEDULE	
4 PERFORMING ORGANIZATION REPORT NUMBER(S)	5 MONITORING ORGANIZATION REPORT NUMBER(S)
6a NAME OF PERFORMING ORGANIZATION: Naval Postgraduate School; 6b OFFICE SYMBOL (If applicable): 3A	7a NAME OF MONITORING ORGANIZATION: Naval Postgraduate School
6c ADDRESS (City, State, and ZIP Code): Monterey CA 93943-5000	7b ADDRESS (City, State, and ZIP Code): Monterey CA 93943-5000
8a NAME OF FUNDING/SPONSORING ORGANIZATION; 8b OFFICE SYMBOL (If applicable)	9 PROCUREMENT INSTRUMENT IDENTIFICATION NUMBER
8c ADDRESS (City, State, and ZIP Code)	10 SOURCE OF FUNDING NUMBERS: PROGRAM ELEMENT NO; PROJECT NO; TASK NO; WORK UNIT ACCESSION NO

11 TITLE (Include Security Classification): Evaluation of Radar Performance Degradation due to Standoff Jamming (Unclassified)

12 PERSONAL AUTHOR(S): Chi, Yoon Kyu

13a TYPE OF REPORT	13b TIME COVERED	14 DATE OF REPORT (Year Month Day)	15 PAGE COUNT
Master's Thesis	FROM ___ TO ___	1992 September	74

16 SUPPLEMENTARY NOTATION: The views expressed in this thesis are those of the author and do not reflect the official policy or position of the Department of Defense or U.S. Govt.

17 COSATI CODES		
FIELD	GROUP	SUB GROUP

18 SUBJECT TERMS (Continue on reverse if necessary and identify by block number): Standoff Jamming, Radar Evaluation

19 ABSTRACT (Continue on reverse if necessary and identify by block number)

This thesis evaluates the performance degradation of Airport Surveillance Radar(ASR-9) due to standoff jamming. ASR-9 data was taken from open literature on this civilian radar. Jammer parameters which are representative of the actual system were postulated to keep the study unclassified. Using these parameters the effect of standoff jamming on detection of targets is evaluated. This evaluation is performed by finding the change in radar SNR due to jamming and computing the probability of detection with and without jamming.

20 DISTRIBUTION/AVAILABILITY OF ABSTRACT	21 ABSTRACT SECURITY CLASSIFICATION
☒ UNCLASSIFIED/UNLIMITED ☐ SAME AS RPT ☐ DTIC USERS	Unclassified
22a NAME OF RESPONSIBLE INDIVIDUAL: G.S. Gill	22b TELEPHONE (Include Area Code): (408) 646-2652; 22c OFFICE SYMBOL: EC/Gi

DD FORM 1473, 84 MAR — 83 APR edition may be used until exhausted. All other editions are obsolete.

SECURITY CLASSIFICATION OF THIS PAGE

Approved for public release; distribution is unlimited.

Evaluation of Radar Performance Degradation Due to Standoff Jamming

by

Chi, Yoon kyu
Lieutenant Colonel, Korea Air Force
B.S., Korean Air Force Academy, 1980

Submitted in partial fulfillment
of the requirements for the degree of

MASTER OF SCIENCE IN SYSTEMS ENGINEERING
(ELECTRONIC WARFARE)

from the

NAVAL POSTGRADUATE SCHOOL
September 1992

Author: Chi yoon kyu
Chi, Yoon Kyu

Approved by: G. S. Gill
G.S. Gill, Thesis Advisor

David C. Jenn
David C. Jenn, Second Reader

Jeffrey B. Knorr, Chairman
Electronic Warfare Academic group

ABSTRACT

This thesis evaluates the performance degradation of Airport Surveillance Radar(ASR-9) due to standoff jamming. ASR-9 data was taken from open literature on this civilian radar. Jammer parameters which are representative of the actual system were postulated to keep the study unclassified. Using these parameters the effect of standoff jamming on detection of targets is evaluated. This evaluation is performed by finding the change in radar SNR due to jamming and computing the probability of detection with and without jamming.

TABLE OF CONTENTS

LIST OF FIGURES

ACKNOWLEDGMENT

I am cordially thankful to God and I wish to express my appreciation to the Korean Air Force for providing the valuable opportunity to study. I would like to personally express my gratitude to my thesis advisor, Professor G.S. Gill, for his patient guidance, dedicated lengthy counsel and continuous support during the preparation of this thesis. Without his help, my effort would never have been successful. I am also very grateful to Professor David C. Jenn, who carefully read and corrected my script.

Finally, I thank to my wife, Jong Ok and daughter, Yong Ju, whose sacrifice and patience have been most supportive during my study at NPGS.

I. INTRODUCTION

A. BACKGROUND

The basic purpose of jamming is to introduce signals into an enemy's electronic system which degrade its performance so that it is unable to perform its intended mission. There are two fundamental categories of jamming: noise jamming and deceptive jamming. In this thesis only noise jamming will be considered. Noise jamming has the effect of obscuring the radar target by immersing it in noise. Noise can be introduced into the victim radar either through the mainlobe or through the sidelobes.

Surveillance radars are vulnerable to jamming in the mainbeam because the jamming gets the large gain of the antenna's mainbeam. When this occurs, the narrow sector in the direction of the jammer will appear as a radial strobe on the PPI display. The direction to the jammer can be determined, but its range and the ranges of any targets are masked by the noise and thus remain unknown. Jamming of the radar through the sidelobes is much more difficult to accomplish because of large jammer effective radiated power(ERP) required to compensate for the low antenna sidelobes. However if sidelobe jamming is successful it denies the radar surveillance in all directions as the entire display can be obliterated. Even the direction of targets and jammer is denied. To avoid such disastrous consequences

radar ECCM features such as sidelobe blanking, sidelobe canceling and low antenna sidelobes are employed to mitigate the effects of the sidelobe jamming.

Radar - ECM is a high stake duel in the modern military warfare in which jammer tries to render the hostile radar useless. Radar in turn needs to operate with minimal effect on performance under jammer attacks.

The subject of radar performance degradation in presence of jamming is of high interest to both radar and jamming communities. There are two approaches to the subject of radar performance evaluation in the presence of jamming. In one approach the jamming threat is estimated by intelligence and the radar performance is computed for the defined threat. In the second approach no jamming threat is assumed, instead the following question is addressed: " What type and amount of jamming will prevent the radar from performing its mission and is such a jammer feasible to build ?" In this thesis, the first approach is taken.

B. OBJECTIVE

The objective of this thesis is to evaluate the effect of jamming on surveillance radar performance. To keep the study unclassified, a representative jamming threat was postulated without using actual data from an existing jammer. The same approach has been taken in the selection of radar parameters. Airport surveillance radar(ASR-9) is of no military significance. Therefore the parameters of this radar are used in the study.

C. RELATED WORK

The maximum detection range of ASR-9 can be computed using the radar equation described by Skolnik[Ref.1], and ASR-9 Radar parameters are taken from Schleher[Ref.4 p:406]. Representative jammer parameters have been assumed.

D. OVERVIEW

This thesis consists of six chapters. Chapter I gives an introduction. Chapter II describes the performance of ASR-9 radar. Chapter III contains standoff jamming tactics and the jamming equations for mainbeam and sidelobe jamming. Chapter IV describes the radar and jammer parameters, and evaluates the radar performance with no jamming, with the mainbeam jamming and with the sidelobe jamming. Chapter V provides the ECCM for mainbeam and sidelobe jamming. Finally, chapter VI summarizes the radar performance degradation due to jamming.

II. RADAR DESCRIPTION

A. SURVEILLANCE RADAR

A surveillance radar is used to maintain cognizance of traffic within a selected area, such as an airport terminal area or air route. A search radar is one which is used primarily for the detection of targets in a particular volume of interest. The difference in definition means that the surveillance radar provides for the maintenance of track files on the selected traffic, while the search radar output may be simply a warning or one time designation of a target for acquisition by a tracker[Ref.6 p:315]. When target track files are maintained by a surveillance radar, the overall radar is usually called a track-while-scan (TWS) radar. This TWS radar develops the target vectors which determine the absolute motion characteristics of the target. The motion characteristics of the target can be used to ascertain the relative threat posed by the target and to predict the future position of the target.

Usually, surveillance radars must provide three-dimensional(3-D)information for air search, and two-dimensional(2-D)information for surface search. The 2-D radar has been the standard even for air search for many years and is still utilized for civilian air traffic control applications. Military applications for surveillance radar are generally being replaced by the newer 3-D radar types. The move towards 3-D radars in military applications is driven by the need to provide height data in high traffic-density situations. A primary function of both 2-D and 3-D surveillance radars

is the estimation of target ground track velocity vectors. The track data is used in military systems for threat identification,threat evaluation, weapon assignment, predicting target position and kill evaluation. In civilian air traffic control systems it is used for traffic control, conflict alert and approach control. The requirements for military systems are more stringent than for civilian systems due to the higher accelerations found in military systems, while in civilian systems the accelerations are lower due to path regularity and pilot collaboration associated with civilian air traffic control operation[Ref.4 pp:265-266]. Most the civilian air traffic control radars are of the 2-D type and ASR-9 is a 2-D radar.

B. THE ASR-9

The S-band ASR-9 is a modern airport surveillance radar designed by Westinghouse for the FAA (Federal Aviation Administration). This radar is installed at more than 100 major airports in the Continental United States and Hawaii. The ASR-9 makes use of the very latest state of the art electronics technology. It operates at S band(2.7-2.9 GHz) with a pulse width of 1.05 μs, a 1.3 degree azimuth beamwidth, an antenna rotation rate of 12.5 rpm, a PRF of the order of 1200 Hz, and a peak transmitter power of 1200 kW. This radar provides the information for aircraft targets within a 60 NM radius of the radar under conditions of ground clutter,weather, angel clutter, interference, and ground vehicular traffic. The ASR-9 transmitter generates coherent RF pulses from a klystron amplifier.

The ASR-9 radar system is a dual channel radar with either channel, when selected, working into a common antenna. One channel of the dual system is active (radiating) while the standby channel is able to assume operational status upon activation of a manual switch. The radar system is designed to operate continuously and unattended over the specified range of service conditions[Ref.10 pp:1-2].

This ASR-9 equipment features a weather channel, moving target detector (MTD), and built-in test equipment(BITE). The weather channel supplies the air traffic controller with real time weather intensity data on his control display. A separate weather channel is used to supply the standard National Weather Service six levels of weather[Ref.12 p:49]. Notable aircraft detection and false alarm control improvements are achieved with MTD processing. The development of MTD has increased the capability of ASR-9 in three areas : 1) detection of aircraft near the airport over heavy ground clutter, 2)detection of aircraft in precipitation, 3) resolution of closely spaced aircraft.

1. MTD (Moving Target Detection)

The MTD has been developed specifically to provide high quality, interference-free data associated with air traffic control systems by the MIT Lincoln Laboratory. Its implementation is based on the application of digital technology. In addition to the MTI, doppler filtering, CFAR-type processing, and a number of censoring techniques are used in the MTD processor.

Figure 2-1 shows a block diagram of the MTD system, which includes a dual fan-beam elevation antenna. Transmission takes place through the lower beam;

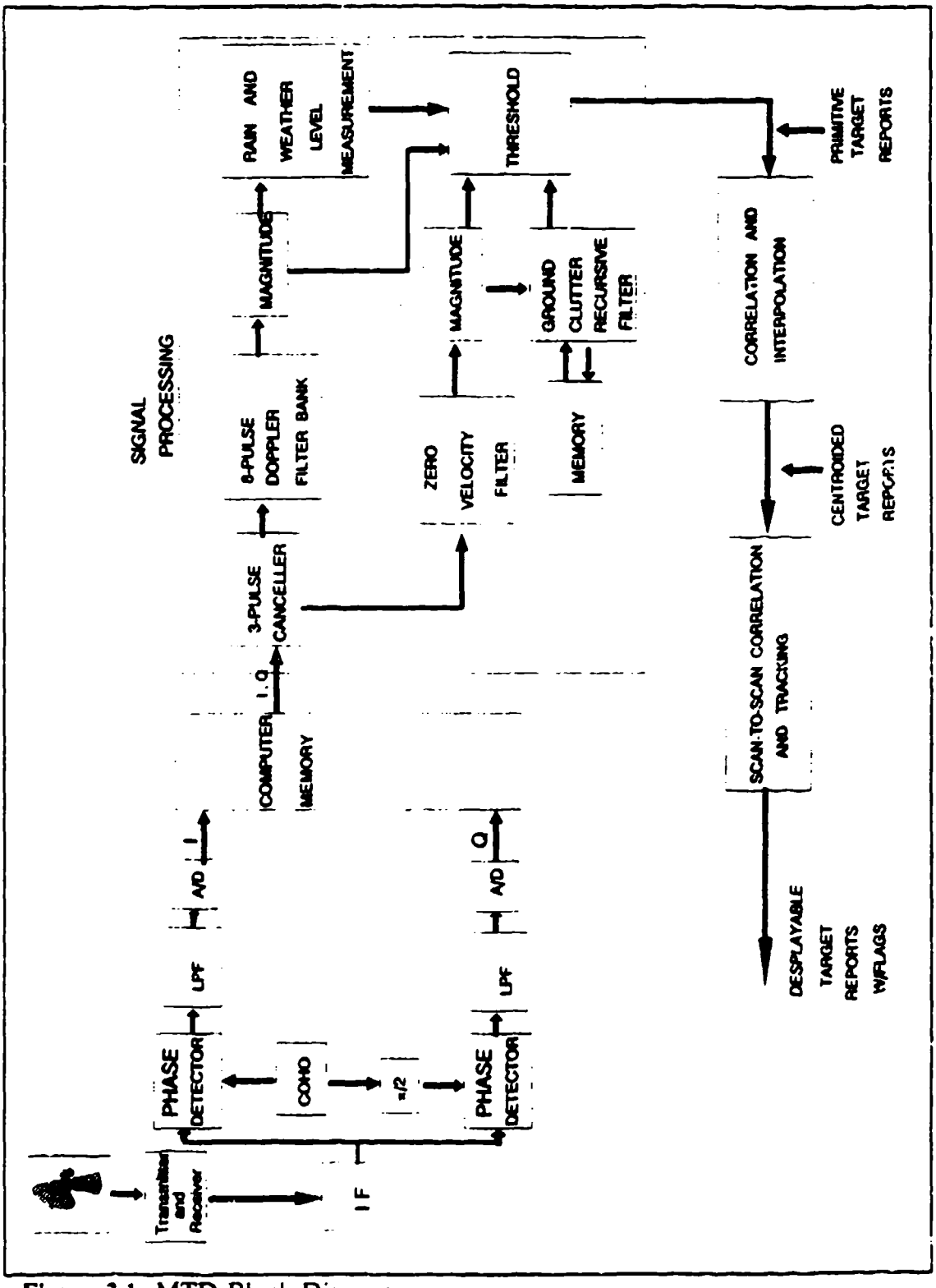

Figure 2.1 MTD Block Diagram

however signals are received through both the beams. The upper beam receives echoes from close range targets with much less clutter from the ground. The lower beam is used for distant targets. Although the antenna normally both radiates and receives vertical polarization, whenever there is heavy precipitation over a significant portion of the coverage, the radar switches to circular polarization. By doing so, the sensor achieves an additional 12 to 20 dB of precipitation-echo rejection. During operation with circular polarization, a switch located on the antenna selects either the weather-channel upper or lower beam. The signal from the selected beam is then passed through a signal rotating joint to the weather-channel receiver.

Signals for target detection pass from the antenna through a sensitivity time control and a low-noise amplifier. After the signals are heterodyned to an intermediate frequency, they are translated to baseband at the output of a linear receiver. This step provides inphase and quadature video signals,which A/D converts into digitized samples[Ref.11 p:364-365]. These samples are then processed in a three pulse canceler and eight-pulse doppler filter bank, which eliminates stationary clutter. The FFT filter bank with weighting is applied in the frequency domain to reduce the filter sidelobes.

A target is declared when the signal crosses a constant false alarm rate(CFAR) threshold. A report is generated for each target. Typically a target report consists of range, azimuth, etc. Then the reports are correlated and centroids are found for the range and azimuth measurements.

The MTD processor performs the following functions:

a. Signal Processing

Signal processing employs special-purpose hardware to cope with the high data rate. Its functions include saturation/interference sensing,velocity domain filtering, constant false alarm rate (CFAR) thresholding, clutter mapping for zero-velocity target processing,and adaptive desensitization in mapped areas defining visible roads and very large amplitude clutter. It can output over thirty thousand primitive target declarations on each scan, the actual number depending on aircraft traffic density, meteorological conditions, presence of birds, etc. An aircraft may produce many primitive target reports per scan,depending on cross section,range, and elevation.

The basic idea of the MTD signal processing is to break the radar coverage into a large number of elemental range-azimuth velocity cells, and to select those cells containing aircraft targets on instantaneous radial velocity and extent characteristics of the real targets as compared to those of extraneous targets including clutter. The ASR-9 MTD processor divides the range coverage(47.5 NM in the original implementation) into 1/16 NM intervals and the azimuth into 3/4 degree intervals for a total 365,000 range-azimuth resolution cells.

$$Resolution\ \ cells = \frac{47.5\ NM}{\frac{1}{16}\ NM} \times \frac{360\ Degree}{\frac{3}{4}\ Degree} = 365{,}000$$

Fig.2-2 shows how the MTD resolution cells are spread through the radar's range, azimuth angle, and doppler coverage.

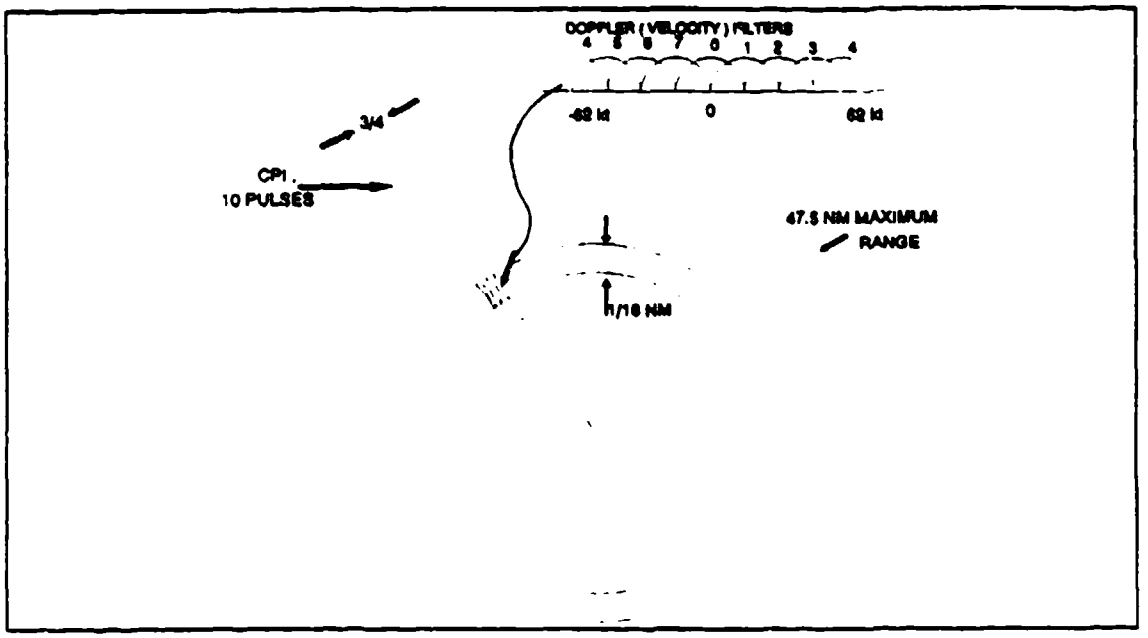

Figure 2.2 MTD Resolution Cell

In each 3/4-degree azimuth interval,ten pulses are transmitted at a constant PRF. On receive, this is called a coherent processing interval(CPI). These ten pulses are processed by the delay-line canceler and 8-pulse doppler filter bank(150 Hz doppler bandwidth). Thus, the radar output is divided into approximately 2,920,000 range-azimuth-doppler cells(8 pulses x 365,000 range-azimuth cell = 2,920,000)[Ref.1 p:127].

The three pulse canceler and the eight pulse doppler filter bank eliminate zero velocity clutter and generate eight overlapping filters covering the doppler. Figure 2.3 shows the frequency response of the three pulse canceler and eight pulse doppler filter bank.

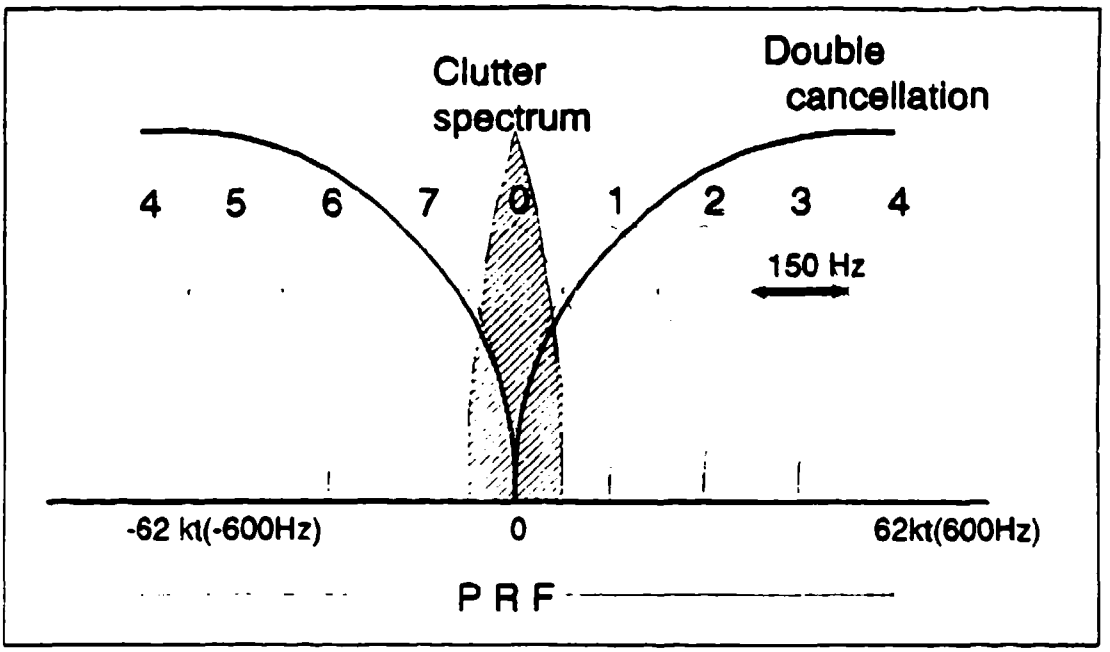

Figure 2.3 The Frequency Response of the Three Pulse Canceler and the Eight Pulse Doppler Filter Bank.

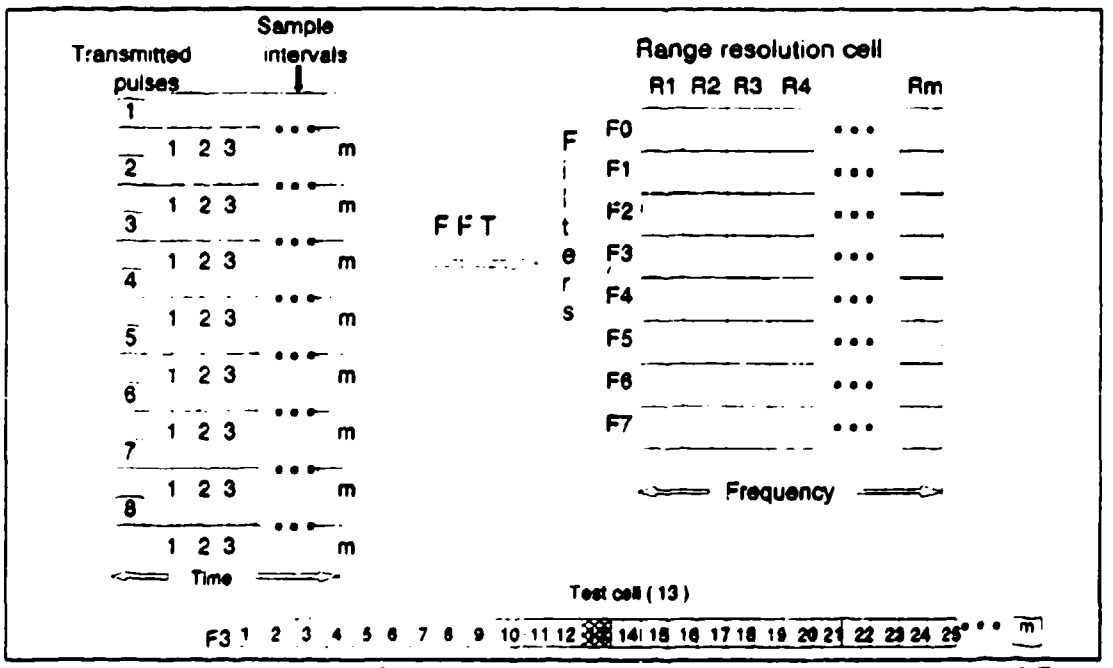

Figure 2.4 The Matrix of Range Resolution Cell and Filter Number at CFAR Detector

The MTD's central functional element is a set of doppler filters, typically 8 or 10 for each range cell.The output of the filters are all individually subjected to thresholds. Figure 2.4 shows the matrix of range resolution cells and doppler filter bank at a CFAR detector.

The threshold for the nonzero-velocity resolution cells (in Figure 2.3 and Figure 2.4, the threshold for filters 2 through 6) are established by the mean-level based on an average of the returns from the same Doppler cell in 16 range cells,eight on either side of the cell of interest. This establishes constant false alarm rate(CFAR) detection. In Figure 2.4, to determine the threshold of the range cell number 13 and the filter number 3, the threshold is established by the mean of range cells 5 to 12 and 14 to 21. The threshold for zero-velocity resolution cells (in Figure 2.3 and Figure 2.4, the threshold for filter 0) is determined by the average of the clutter values that were observed in the subject range cell over 10 to 20 scans. The threshold for filters 1 and 7 adjacent to the zero-velocity in Figure 2.3 are the greater of a mean level threshold from the 16 range cells and a clutter threshold from the clutter map.[Ref.1 p:128-129]

To obtain acceptable performance in conditions of rain and ground clutter interference, the MTD uses a set of eight finite impulse response filters for each range cell. Two pulse repetition intervals are used to prevent the masking that occurs when rain clutter obscures a target. The PRF's differ by about 20 %.

b. Correlation and Interpolation

The correlation and interpolation(C&I) processing correlates primitive reports in the same scan that are associated with the same target using range/azimuth adjacency, and interpolates to develop the centroid of measurement variables(range, azimuth, velocity and amplitude). It also performs adaptive second-level thresholding, and flags each target report with a quality/confidence indicator before transmitting them to the third-level of processing(track filtering). The C&I processing attempts to produce a single target report for each moving aircraft target within the radar coverage, on each scan of the antenna, while adaptively limiting the false alarms to fewer than 60 per scan.

c. Scan-to-Scan Correlation and Tracking

The scan-to-scan correlation and tracking processing uses target scan-to-scan history to "track" moving aircraft targets while filtering out those target reports that are not associated with moving aircraft. Approximately 98 % of the aircraft reports entering this processor are transmitted for display, while fewer than one false alarm per scan are transmitted for display under most conditions.

2. Weather Channel

The weather channel provides superior performance by producing smooth, stable contours of storm intensity. Unlike the weather data produced by MTI, the ASR-9 contours are not biased due to the following factors: the sensor's circuitry, circular polarization, antenna high-low beam selection, and sensitivity time control.In

ASR-9, a programmable range dependent threshold compensates for the above factors and reduces the estimate bias that occurs from the partial filling of the radar beam by the vertical extent of the storm.

Figure 2.5 contains a block diagram of the ASR-9 weather processor.

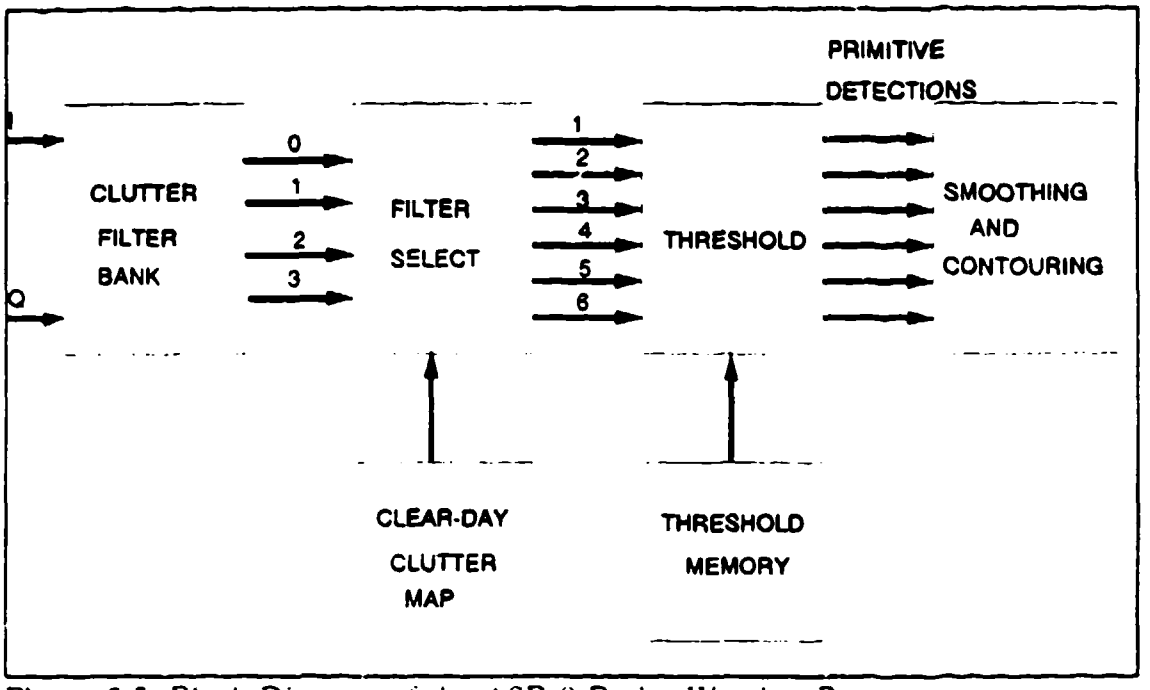

Figure 2.5 Block Diagram of the ASR-9 Radar Weather Processor

Digitized quadrature video signals pass through four parallel clutter filters:one all pass and three notch type. A set of four filters effectively eliminates ground clutter. The attenuating effect of these filters on storm echoes that have low radial velocities is mitigated by a ground clutter map that was made on a clear day. The clear day map can be used to select, on a range cell by range cell basis, the output of the least attenuating filter for each desired weather level. Spatial and temporal smoothing provides stable contours of precipitation regions.

III. DEPLOYMENT OF STANDOFF JAMMING AND JAMMING EQUATION

Noise jamming has the advantage against surveillance radars in that little need be known about the victim radar's parameters except its frequency range[Ref.4 p:111]. A convenient classification of noise jamming is by the ratio of the jamming bandwidth to the acceptance bandwidth of the victim equipment. If the ratio is large, it is called barrage jamming. However if the ratio is small, then it is called spot jamming. The bandwidth of barrage noise jammer extends over a large frequency band which includes the entire tuning band of the radar. Barrage noise jammer bandwidth is typically 10% of the radar RF frequency extending over several hundred megahertz.

The operational categories of jamming include escort jamming, self-protect jamming, stand-off jamming. Only standoff jamming is discussed in this.

A. STANDOFF JAMMING TACTICS AND DEPLOYMENT

The stand-off jammer on a heavier and slower platform can carry a higher power jamming transmitter and a higher gain antenna as compared to an attack aircraft[Ref.2 p: 6]. The ERP of a single transmitter/antenna combination may be in the range of +50 dBW to + 100 dBW. This high ERP overcomes the propagation loss of a larger jammer range and enables it to inject jamming power through the radar antenna's sidelobes. Several transmitters may be aboard a single aircraft, with one or more of the transmitters dedicated to jam a given type or class of radars(e.g.,surveillance,tracking,or imaging radars)[Ref.13 p:12-4].

Usually, the jamming aircraft may orbit an elongated racetrack course,the long axis of which is normal to the line-of-sight(LOS) to the area targeted for jamming behind the forward line of troops(FLOT),and transmit from one of two antennas toward the victim radars. With two or more jamming aircraft simultaneously on orbit, one can cover for the other as the latter executes the turn at either end of the racetrack[Ref.2 p:2]. A typical stand-off radar jammer employs an ESM system with direction finding capability to locate threat radars.

B. JAMMING EQUATIONS

In this section we develop the equations for standoff jamming. A standoff jammer can jam either through the mainbeam or the sidelobes of victim radar's antenna to reduce its detection range. Both cases will be considered. The calculation depends upon finding the change in radar signal-to-noise ratio(SNR) due to the jamming. A reduced SNR would result in a smaller detection range as compared to the normal detection range of the radar.

1. Mainbeam Jamming

a. Radar Range Reduction

The signal to interference(S/I) at the CFAR detector in the presence of a jammer will depend upon radar and jammer parameters and can be written as

$$\frac{S}{I} \triangleq \frac{S}{J+N} \tag{3.1}$$

where

S is target signal power

J is jamming power

N is thermal noise

S/I in the above equation can be written in two ways as

$$\frac{S}{I} = \frac{1}{\frac{1}{\frac{S}{N}} + \frac{J}{S}} \tag{3.2}$$

$$\frac{S}{I} = \frac{\frac{S}{N}}{1 + \frac{J}{N}} \tag{3.3}$$

In this thesis, the second method for radar range reduction is considered. It may be noted that S/N is normal SNR at the CFAR detector. This quantity can be computed by using normal radar range equation.

By taking 10 log of Equation 3.3 it can be rewritten as

$$\left(\frac{S}{I}\right)_{dB} = \left(\frac{S}{N}\right)_{dB} - \left(\frac{J}{N}+1\right)_{dB} \tag{3.4}$$

and rearranging

$$\left(\frac{S}{N}\right)_{dB} - \left(\frac{S}{I}\right)_{dB} = \left(\frac{J}{N}+1\right)_{dB} \tag{3.5}$$

It may be noted that the left hand side of the above equation represents a loss in radar signal-to-noise ratio (in dB) due to jamming. Thus the decrease in S/N can be determined by computing $(1 + J/N)_{dB}$. This loss of $(1 + J/N)_{dB}$ in the normal SNR due to jamming can be represented as reduction in detection range. J/N can be determined by computing jammer power and thermal noise in the radar receiver.

Jammer power J in the mainbeam is given by

$$J = \frac{P_j G_j G_r \lambda^2}{(4\pi R_j)^2 L_j} \left(\frac{B_r}{B_j}\right) K_j \tag{3.6}$$

where

P_j is jammer power in watts

G_j is jammer antenna gain

L_j is jammer loss

R_j is radar range to jammer

B_r is radar bandwidth

B_j is jammer bandwidth

K_j is jammer waveform gain in the radar signal processor

Receiver thermal noise N is given by

$$N = k T_o F B_r \tag{3.7}$$

where

k is Boltzman's constant of magnitude 1.38×10^{-23}

T_o is room temperature of 290°F

F is radar receiver noise figure

From Equation 3.6 and 3.7, J/N is given by

$$\frac{J}{N} = \frac{P_j G_j G_r \lambda^2}{(4\pi R_j)^2 L_j} \frac{1}{k T_o B_r F} \left(\frac{B_r}{B_j}\right) K_j \tag{3.8}$$

It may be noted that the above equation is valid only for noise jammers (not, for example, for coherent jammers which will have some processing gain).

Loss in radar SNR due to jamming is computed as

$$L_j = 1 + \frac{J}{N}$$

The maximum radar detection range(R_2) under jamming conditions is given by

$$R_2 = (\frac{1}{L_J})^{\frac{1}{4}} R_1 \tag{3.9}$$

where

R_1 is maximum radar detection range under normal conditions.

R_2 is maximum radar detection range under jamming conditions.

The following table shows examples of range reduction for assumed losses.

Loss(dB)	L_J	$(1/L_J)^{1/4}$	Range reduction
1	$10^{0.1}$ = 1.259	0.94	6 %
2	$10^{0.2}$ = 1.585	0.89	11 %
3	$10^{0.3}$ = 1.995	0.84	16 %
5	$10^{0.5}$ = 3.162	0.74	24 %
10	10^{1} = 10	0.56	44 %
15	$10^{1.5}$ = 31.6	0.42	58 %
20	10^{2} = 100	0.31	69 %

b. Burn-through Range

In free space the radar echo power returned from a target varies inversely as the fourth power of the range, while power received at the radar from a jammer varies inversely with the square of the target range. Therefore, as range decreases, radar

echo power from the target increases more rapidly than does received energy from the jammer. Inevitably a point is reached where the energy received from a noise jammer is no longer great enough to hide the target echo. This range is called the burn-through range[Ref. 14 p:54].

To compute the burn-through range we need to compute J/S first. The signal power into the radar antenna is given by

$$S = \frac{P_t G_t G_r \sigma \lambda^2}{(4\pi)^3 (R_T)^4 L_s} PCR\, N_p \qquad (3.10)$$

where

P_t is peak transmitter power in watts

G_t is transmit antenna gain

G_r is radar antenna gain

σ is target radar cross section

L_s is signal loss in the radar

R_T is radar range to target

λ is radar signal wavelength

PCR is pulse compression ratio

N_p is Number of pulses integrated (FFT gain)

Jammer power J in the radar receiver through the mainbeam of the radar antenna is given by

$$J = \frac{P_j G_j G_r \lambda^2}{(4\pi R_j)^2 L_j} \left(\frac{B_r}{B_j}\right) K_j \tag{3.11}$$

It may be noted that B_r/B_j does not exceed unity even if B_j is less than B_r. Therefore, J/S can be written as

$$\frac{J}{S} = \frac{P_j G_j}{P_t G_t} \frac{4\pi}{\sigma} \frac{(R_T)^4}{(R_j)^2} \frac{B_r}{B_j} \frac{K_j}{PCR\, N_p} \frac{L_s}{L_j} \tag{3.12}$$

Burn-through range from above can be written as

$$R = \left(\frac{P_t G_t}{P_j G_j} \frac{\sigma (R_j)^2}{4\pi} \frac{B_j}{B_r} \frac{PCR\, N_p}{K_j} \frac{L_j}{L_s} \left(\frac{J}{S}\right)\right)^{\frac{1}{4}} \tag{3.13}$$

(J/S) in the above equation is computed from the specified probability of detection.

2. Sidelobe Jamming

a. Radar Range Reduction

When the stand-off jammer jams through the sidelobes of the victim radar's antenna, it suffers a disadvantage equal to the radar's mainlobe to sidelobe gain ratio. The effect of sidelobe jamming on the radar performance can be determined in the same manner as for the mainbeam jamming case except for the computation of jammer to

noise (J/N) ratio. The sidelobe jammer power J in the receiver of the victim radar is given by

$$J = \frac{P_j G_j G_{sl} \lambda^2}{(4\pi R_j)^2 L_j} \frac{1}{SLC} \left(\frac{B_r}{B_j}\right) K_j \qquad (3.14)$$

where

G_{sl} is sidelobe gain of radar receiver.

SLC is sidelobe cancellation ratio if any.

If $B_r < B_j$, then $B_r/B_j = B_r/B_j$.

If $B_r \geq B_j$, then $B_r/B_j = 1$.

K_j is jammer signal processing gain if any. It will be unity for noise jamming.

J/N can be written as

$$\frac{J}{N} = \frac{P_j G_j G_{sl} \lambda^2}{(4\pi R_j)^2 L_j} \frac{1}{k T_o B_r F} \frac{1}{SLC} \left(\frac{B_r}{B_j}\right) K_j \qquad (3.15)$$

Therefore, range reduction can be computed using Equation 3.9.

b. Burn-through Range

The signal power into the radar receiver is given by

$$S = \frac{P_t G_t G_r \sigma \lambda^2}{(4\pi)^3 (R_T)^4 L_s} PCR\, N_p \qquad (3.16)$$

Sidelobe jamming power J in the radar receiver is given by

$$J=\frac{P_j G_j G_{sl} \lambda^2}{(4\pi R_j)^2 L_j} \left(\frac{B_r}{B_j}\right) K_j \tag{3.17}$$

J/S for the sidelobe jammer at the CFAR detector can be written as

$$\frac{J}{S} = \frac{P_j G_j}{P_t G_t} \frac{4\pi}{\sigma} \frac{(R_T)^4}{(R_j)^2} \frac{B_r}{B_j} \frac{K_j}{PCR\, N_p} \frac{L_s}{L_j} \frac{G_{sl}}{G_r} \tag{3.18}$$

From above, burn-through range can be written as

$$R = \left(\frac{P_t G_t}{P_j G_j} \frac{\sigma (R_j)^2}{4\pi} \frac{B_j}{B_r} \frac{PCR\, N_p}{k_j} \frac{L_j}{L_s} \frac{G_r}{G_{sl}} \left(\frac{J}{S}\right)\right)^{\frac{1}{4}} \tag{3.19}$$

(J/S) in the above equation is computed from the specified probability of detection.

IV. THE EVALUATION OF ASR-9 RADAR PERFORMANCE

In this chapter, the ASR-9 radar and the jammer parameters are specified. The radar probability of detection is determined as a function of target(to radar) range without jamming. Then the same computation is performed with both mainbeam and sidelobe standoff jamming. Both barrage and spot noise jamming are considered. Burn-through ranges are determined for both mainbeam and sidelobe jamming.

A. ASR-9 RADAR AND JAMMER PARAMETERS

1. ASR-9 Radar Parameters

ASR-9 radar has the following parameters.

Peak power (P_t)	= 1200 kw (60.79 dBW)
Antenna Gain ($G = G_t = G_r$)	= 33.5 dB
Sidelobe gain of radar receiver (G_{sl})	= 3.5 dB
Radiated Frequency (f)	= 2.9 GHz
Wavelength(λ)	= 10.35 cm (10.15 dBcm)
Pulse Width (τ)	= 1.05 μs
Antenna Azimuth Beamwidth (θ)	= 1.3 degree
Rotation Rate	= 12.5 rpm
Scan rate	= 75 degree/sec
Pulse Repetition Frequency(PRF)	= 1200 pps
Noise Figure (F)	= 5 dB

Target radar cross section (σ) = 1 m^2 (0 dBsm)

Doppler bandwidth (B_{Dopp}) = 150 Hz

Pulse Compression Ratio(PCR) = 0 dB

Probability of detection (P_D) = 0.9

Probability of false alarm (P_{FA}) = 10^{-6}

Total system Losses (L) = 12 dB

System losses are broken down as follows.

Transmitter	= 2 dB
Receiver	= 2 dB
Mismatch	= 1 dB
Integrator	= 1 dB
Collapsing	= 1 dB
Beam shape	= 3 dB
MTI	= 2 dB

Radar bandwidth(B) = 9.52 x 10^5 Hz (59.8 dBHz)

Number of pulses(n) = (beamwidth/scan rate) x PRF

= 21 (13.22 dB)

Integration efficiency($E_i(n)$) = 1 for coherent integration

Elevation Beamwidth (-3 dB) = 4.8 degree (minimum)

2. Jammer Parameters

Assume jammer parameters as given below

Jammer ERP	= 20 dBW
Range between standoff jammer and radar(R_j)	= 50 NM
Jammer loss(L_j)	= 0 dB
Jammer bandwidth(B_j) ;	
Spot noise jamming	= 10 MHz
Barrage noise jamming	= 300 MHz
Jammer signal processor gain(K_j)	= 0 dB
Radar sidelobe cancellation ratio(SLC)	= 0 dB

B. MATHEMATICAL EVALUATION

1. Radar Performance Evaluation without Jamming

Radar performance under normal conditions is usually computed using professionally written computer programs, but the basic steps of the computation are outlined in this section. Maximum detection range for ASR-9 will be determined by coherently integrating the pulses over one scan.

For target model case 1(swerling 1), the echo pulses received from the target on any one scan are of constant amplitude throughout the entire scan, but are independent from scan to scan.

a. For case 1, P_D, and P_{FA} are related by

$$P_D = (P_{FA})^{\frac{1}{(\frac{S}{N})_1 + 1}} \tag{4.1}$$

which can be rewritten as

$$(\frac{S}{N})_1 = \frac{\log P_{FA}}{\log P_D} - 1 \tag{4.2}$$

where $(S/N)_1$ is single pulse SNR required to achieve stated P_D and P_{FA}.

With $P_D = 0.9$ and $P_{FA} = 10^{-6}$, $(S/N)_1 = 130.13$ (21.1 dB)

b. Maximum detection range(R_{max}) is given by

$$R_{max}^4 = \frac{P_t G^2 \lambda^2 \sigma n E_i(n) PCR}{(4\pi)^3 (\frac{S}{N})_1 k T B F L} \tag{4.3}$$

Equation 4.3 can be written in logarithmic form in mixed units as given below

$$4(R)_{dBnm} = (P_t)_{dBW} + 2(G)_{dB} + 2(\lambda)_{dBcm} + (\sigma)_{dBsm} + (n E_i(n))_{dB} - (S/N)_{1\,dB} - (B)_{dBHz} - (F)_{dB} - (L)_{dB} + 0.3 \tag{4.4}$$

c. Substituting the values of radar parameters in the left hand side

$$4(R)_{dBnm} = 60.79 + 2 \times 33.5 + 2 \times 10.15 + 0 + 13.22 - 21.14 - 59.8 - 5 - 12 + 0.3$$

$$= 63.67$$

and therefore

R_{max} = 39.05 NM

d. Thus, the maximum de ection range of ASR-9 under normal conditions (for case 1 RCS model with P_D of 0.9 and P_{FA} of 10^{-6}) is 39.05 NM.

e. From Equation 4.2 and 4.3

$$R_{max}^4 = \frac{P_t G^2 \lambda^2 \sigma n E_i(n) PCR}{(4\pi)^3 \left(\frac{\log P_{FA}}{\log P_D} - 1\right) k T B F L} \tag{4.5}$$

f. Equation 4.5 gives R_{max} for any P_D. Using this equation to plot P_D vs range results in Figure 4.1. Previously defined radar parameters of ASR-9 are used with P_D as a variable parameter. It can be seen from the Figure 4.1 that as P_D increases, the detection range decreases, which is expected.

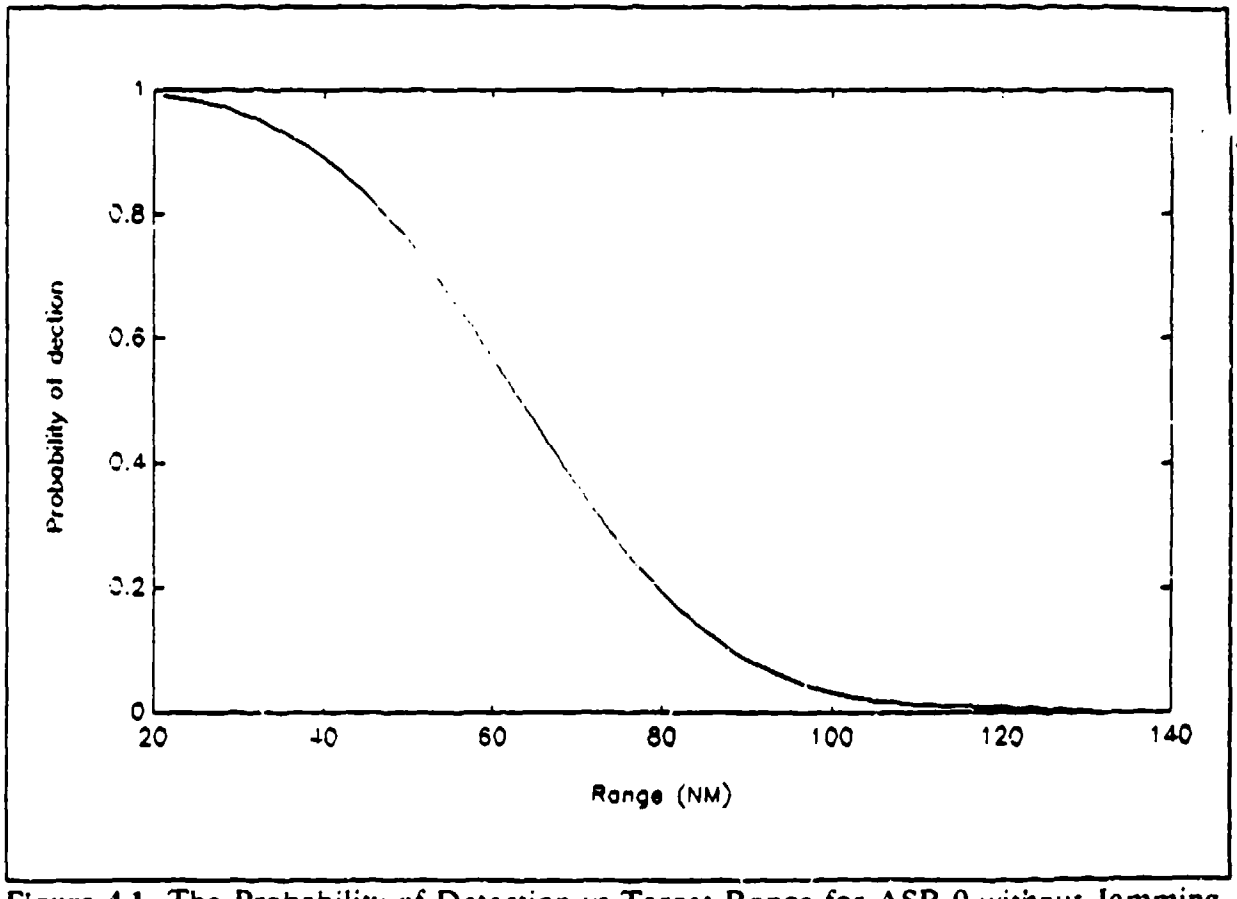

Figure 4.1 The Probability of Detection vs Target Range for ASR-9 without Jamming

Figure 4.1 also shows the 39.05 NM maximum range at 0.9 probability of detection without jamming.

2. Radar Performance Evaluation with Mainbeam Jamming

a. Maximum Detection Range with Barrage Jamming

To compute radar detection range in jamming, first compute J/N

$$\frac{J}{N} = \frac{P_j G_j G_r \lambda^2}{(4\pi R_j)^2 L_j} \frac{1}{k T_o B_r F} \left(\frac{B_r}{B_j}\right) \tag{4.6}$$

The logarithmic form of the equation is as follows

$$(J/N)_{dB} = (ERP_j)_{dBW} + (G_r)_{dB} + 2(\lambda)_{dBm} - 2(R_j)_{dBm} + (B_r)_{Hz} - (B_j)_{Hz} - (L_j)_{dB} - (B_r)_{dB} - F + 181.993 \tag{4.7}$$

By substituting radar and jammer parameters

$$(J/N)_{dB} = 20 + 33.5 + 2(-9.85) - 2(10 \log(1852 \times R_j)) - 84.77 - 5 + 181.993$$

$$= 126.02 - 20 \log(1852 \times R_j) \tag{4.8}$$

The loss in SNR due to jamming is given by

$$L_J = 1 + \frac{J}{N} = 1 + 10^{\frac{\left(\frac{J}{N}\right)_{dB}}{10}} \tag{4.9}$$

The radar detection range(R_2) under jamming conditions is

$$R_2 = \left(\frac{1}{L_j}\right)^{\frac{1}{4}} R_1 \qquad (4.10)$$

where

R_1 is maximum radar detection range under normal conditions(without jamming).

R_2 is maximum radar detection range under jamming conditions.

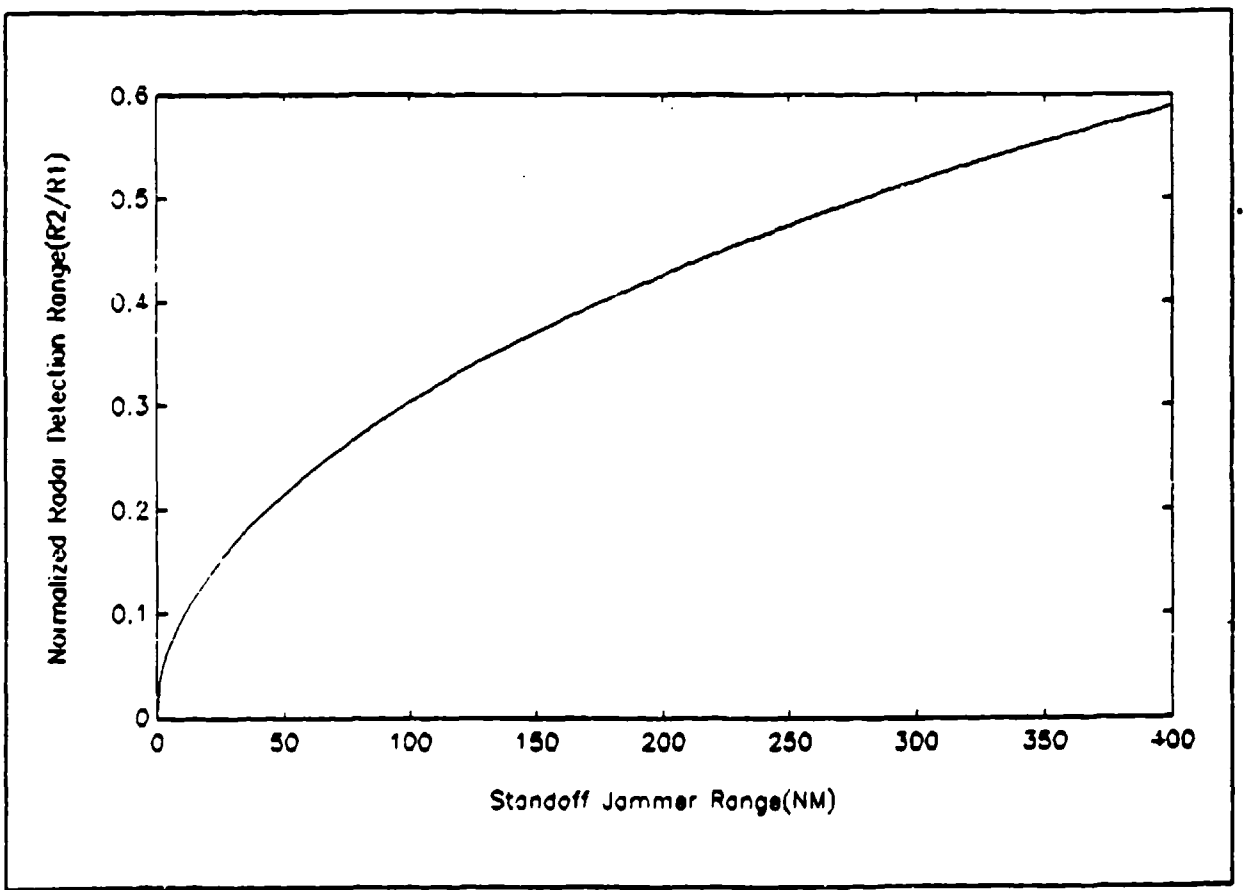

Figure 4.2 Normalized Radar Detection Range(R_2/R_1) vs Standoff Jammer Range(R_j) for the Mainbeam Barrage Jamming.

Using Equations 4.8,4.9 and 4.10, normalized radar detection range(R_2/R_1) is plotted as a function of radar range to jammer(R_j). Figure 4.2 shows a normalized detection range

of 0.22 at 50 NM of radar range to jammer. Thus normal radar detection range is reduced by factor of 78 %. For the specific case of P_D = 0.9, R_j = 50NM the detection range R_2 under jamming is obtained as

$R_2 = 0.22 \times R_1$

= 8.40 NM (for R_1 = 39.05 NM)

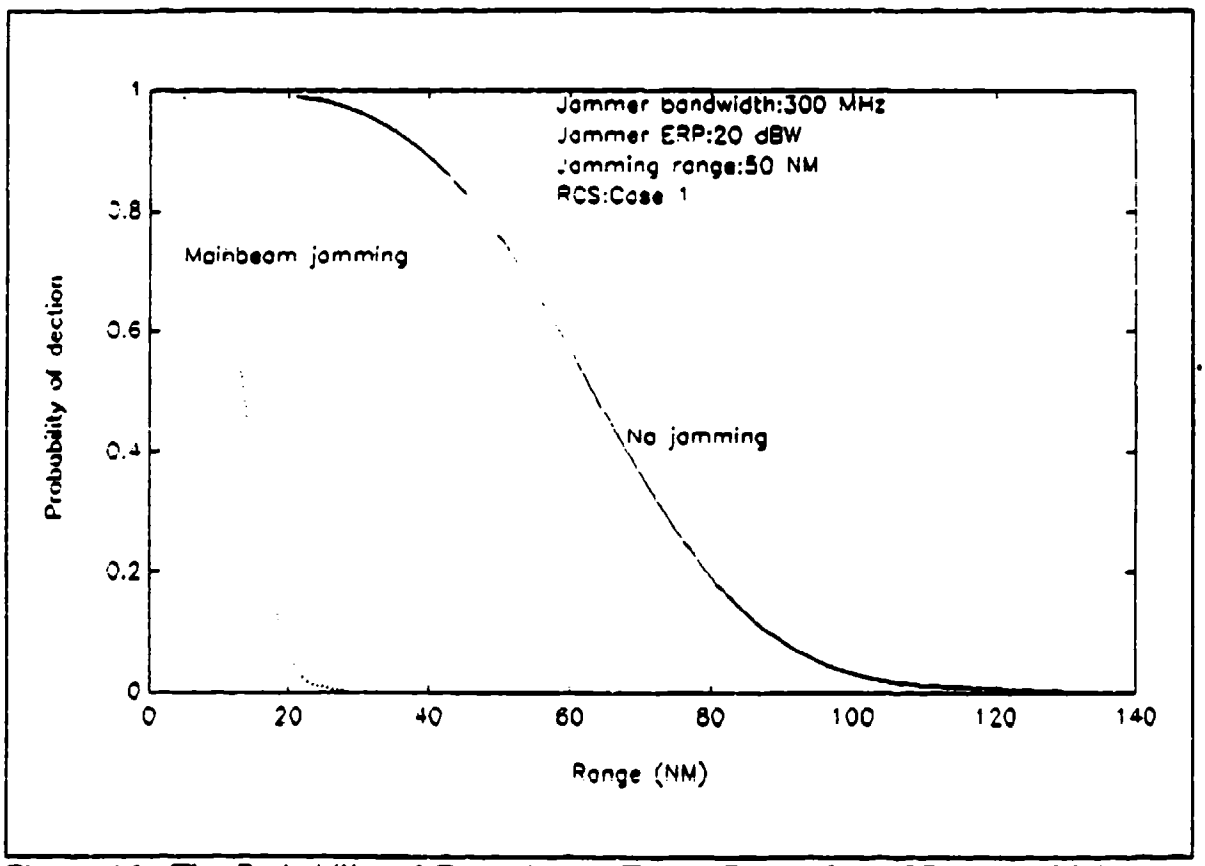

Figure 4.3 The Probability of Detection vs Target Range for ASR-9 with Mainbeam Barrage jamming.

To determine the detection range under jamming and all values of P_D for radar to jammer range of 50 NM, the following formula can be used

$$R_2 = 0.22 \times \left(\frac{P_t\, G^2\, \lambda^2\, \sigma\, n\, E_i(n)\, PCR}{(4\pi)^3 \left(\frac{\log P_{FA}}{\log P_D} - 1\right) k\, T\, B\, F\, L}\right)^{\frac{1}{4}} \qquad (4.11)$$

For the assumed radar parameters, the results are plotted in Figure 4.3.

b. Maximum Detection Range with Spot Jamming

Spot noise jammer parameters are as follows.

Bandwidth = 10 MHz

Jammer ERP = 20 dBW

Jamming range = 50 NM

By substituting radar and jammer parameters in Equation 4.6, the ratio $(J/N)_{dB}$ is

$$(J/N)_{dB} = 20 + 33.5 + 2(-9.853) - 2(10 \log(1852 \times R_j)) - 70 - 5 + 181.993$$

$$= 140.79 - 20 \log(1852 \times R_j) \qquad (4.12)$$

Using Equations 4.12,4.9,and 4.10, a graph of normalized detection range(R_2/R_1) vs jamming distance(R_j) is constructed. Figure 4.4 shows 9 % at a 50 NM range to jammer.

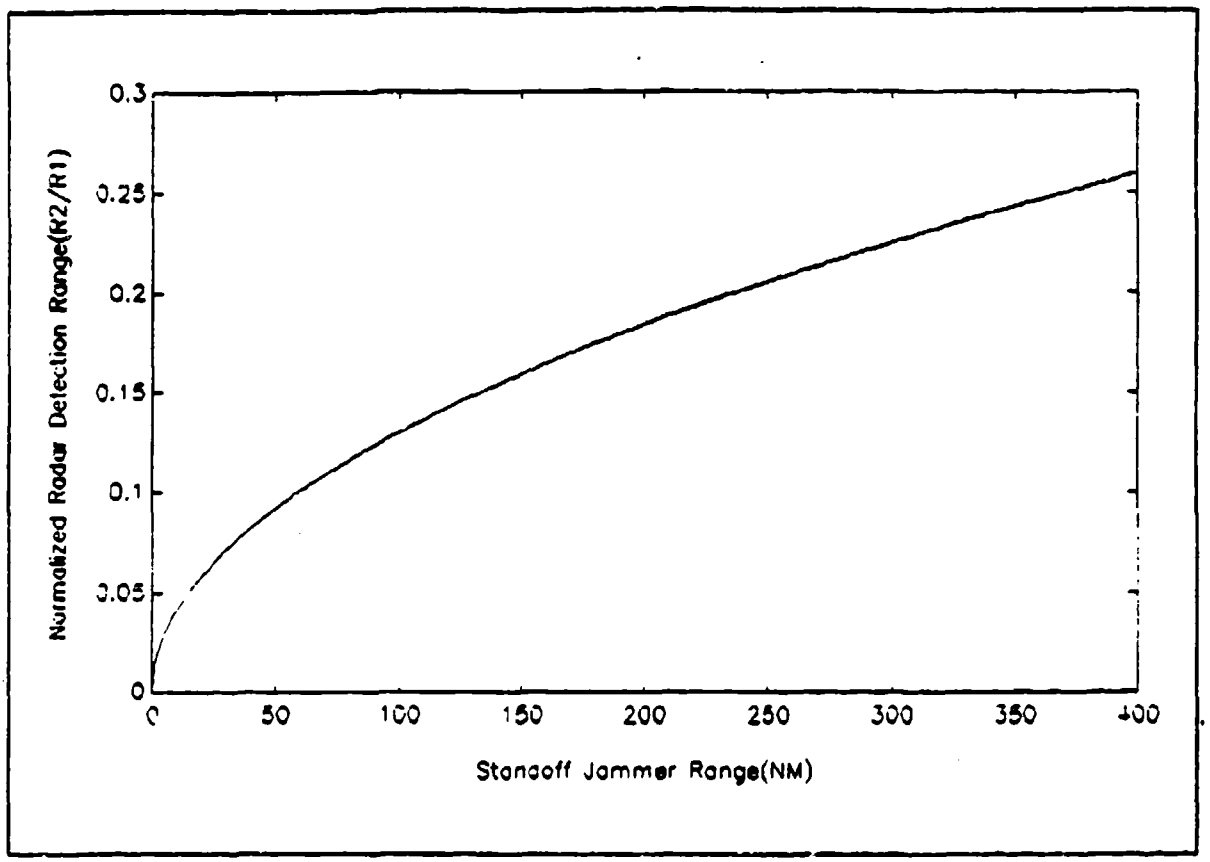

Figure 4.4 Normalized Radar Detection Range vs Standoff Jammer Range for the Mainbeam Spot Jamming

For the specific case of $P_D = 0.9$, $P_{FA} = 10^{-6}$ and $R_j = 50$NM, the detection range R_2 under jamming is obtained as

$R_2 = 0.09 \times R_1$

$= 3.59$ NM

To determine detection range under jamming for all values of P_D, use the following formula

$$R_2 = 0.09 \times \left(\frac{P_t G^2 \lambda^2 \sigma n E_i(n) PCR}{(4\pi)^3 \left(\frac{\log P_{FA}}{\log P_D} - 1 \right) k T B F L} \right)^{\frac{1}{4}} \qquad (4.13)$$

The results are plotted in Figure 4.5.

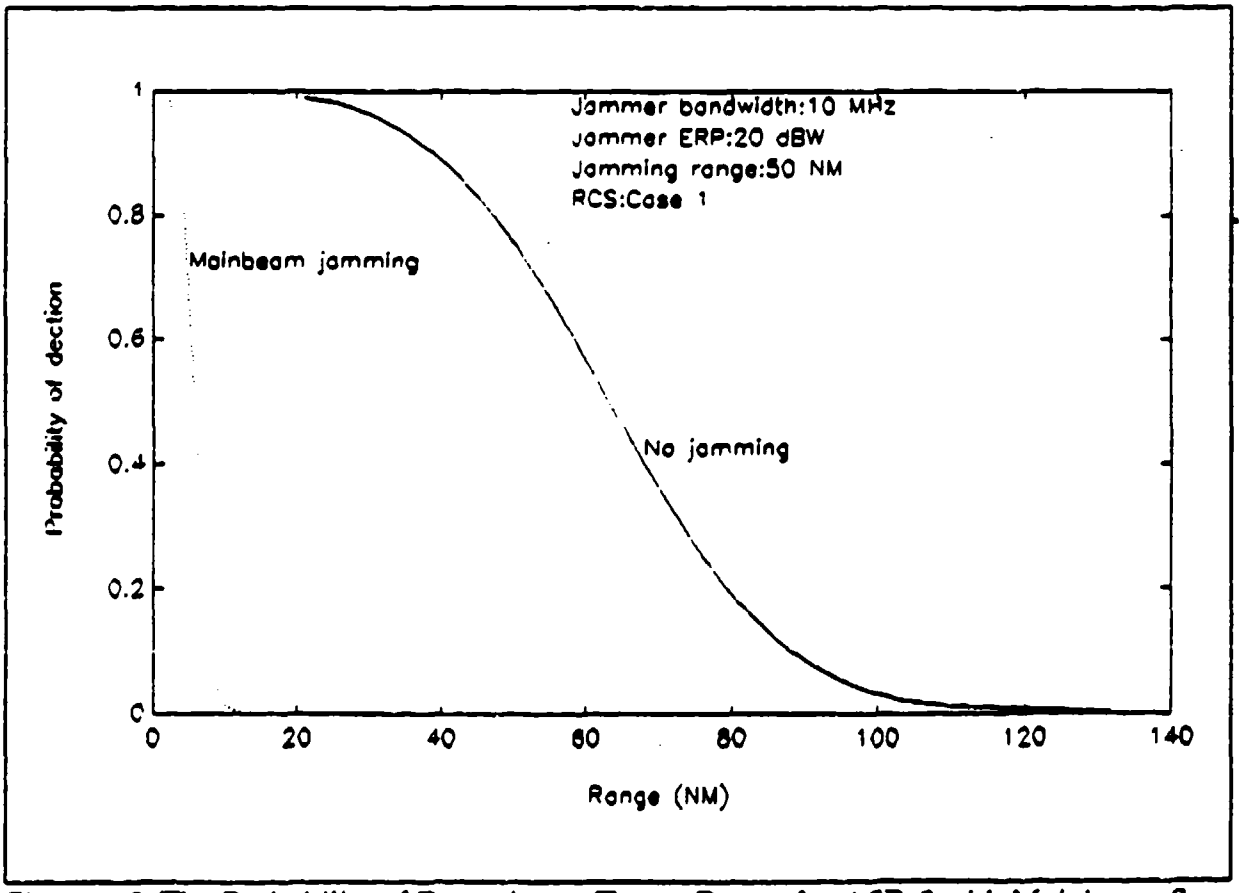

Figure 4.5 The Probability of Detection vs Target Range for ASR-9 with Mainbeam Spot Jamming.

c. *Burn-through Range and Crossover Range*

The range at which the radar and jammer powers are equal (J/S = 1) is often referred to as the jammer crossover range. The term "burn-through range" has been generally used to denote a range at which targets can be detected more reliably than indicated by crossover range. In this thesis, the range at which target can be detected with a 50 % probability of detection in the presence of jamming will be called " burn-through range ".

These ranges are calculated for mainlobe jamming from the following equation

$$R = \left(\frac{P_t G_t}{P_j G_j} \frac{\sigma (R_j)^2}{4\pi} \frac{B_j}{B_r} \frac{PCR\, N_p}{K_j} \frac{L_j}{L_s} \left(\frac{J}{S}\right)\right)^{\frac{1}{4}} \qquad (4.14)$$

In logarithmic form

$$4R_B = (P_t)_{dBW} + (G_t)_{dB} - (P_j)_{dB} - (G_j)_{dB} + (\sigma)_{dBsm} + 2(R_j)_{dbm} - 10.992 + (B_j)_{Hz} - (B_r)_{Hz} + (PCR\ N_p)_{dB} - (K_j)_{dB} + (L_j)_{dB} - (L_s)_{dB} + (J/S)_{dB} \qquad (4.15)$$

Substituting the relevant radar and jammer parameters(with jammer bandwidth of 300 MHz, J/S = 1) in the above equation

$(R_C)_{dB}$ = (60.79 + 33.5 - 20 + 2(49.67) - 10.99 + 24.99 + 13.22 - 12)/4 = 47.21 dB

R_C = 52,632 m = 28.42 NM for the mainlobe jamming.

Now compute J/S required for 50 % probability of detection(P_D). From Equation 3.2, in the presence of jamming

$$\frac{J}{S} = \frac{1}{\frac{S}{I}} - \frac{1}{\frac{S}{N}} \tag{4.16}$$

where S/I is signal-to-interference ratio required for P_D of 50 % and S/N is signal-to-noise ratio for P_D of 90 %. Solving gives

$$\frac{S}{I} = \frac{\log P_{FA}}{\log P_D} - 1 \tag{4.17}$$

For P_D = 0.5 and $P_{FA} = 10^{-6}$, S/I = 18.93. From Equation 4.2, the SNR under normal conditions(P_D = 0.9, $P_{FA} = 10^{-6}$) was computed before as 130.13. Substituting the values of S/N and S/I in Equation 4.16, gives

$$\frac{J}{S} = \frac{1}{18.93} - \frac{1}{130.13} = 0.045 \tag{4.18}$$

Substituting this value of J/S in Equation 4.15, we obtain R_B = 43.85 dB which gives R_E = 24,246 m or 13 NM for the mainbeam jamming.

3. Radar Performance Evaluation with Sidelobe Jamming

a. Maximum Detection Range with Barrage Jamming

For sidelobe barrage jamming, compute J/N(for B_j of 300 MHz) as follows

$$\frac{J}{N} = \frac{P_j G_j G_{sl} \lambda^2}{(4\pi R_j)^2 L_j} \frac{1}{k T_o B_r F} \left(\frac{B_r}{B_j}\right) \tag{4.19}$$

The logarithmic form of the equation is

$$(J/N)_{dB} = (ERP_j)_{dBW} + (G_{sl})_{dB} + 2(\lambda)_{dBm} - 2(R_j)_{dBm} + (B_r)_{Hz} - (B_j)_{Hz} - (L_j)_{dB} - (B_r)_{dB} - F + 181.993 \tag{4.20}$$

By substituting radar and jammer parameters, we obtain $(J/N)_{dB}$ as given below

$$(J/N)_{dB} = 20 + 3.5 + 2(-9.85) - 2(10 \log(1852 \times R_j)) - 84.77 - 5 + 181.993$$

$$= 96.02 - 20 \log(1852 \times R_j) \tag{4.21}$$

The loss in SNR due to jamming is given by

$$L_J = 1 + \frac{J}{N} = 1 + 10^{\frac{(\frac{J}{N})_{dB}}{10}} \tag{4.22}$$

Therefore, the radar detection range(R_2) under jamming is

$$R_2 = \left(\frac{1}{L_J}\right)^{\frac{1}{4}} R_1 \qquad (4.23)$$

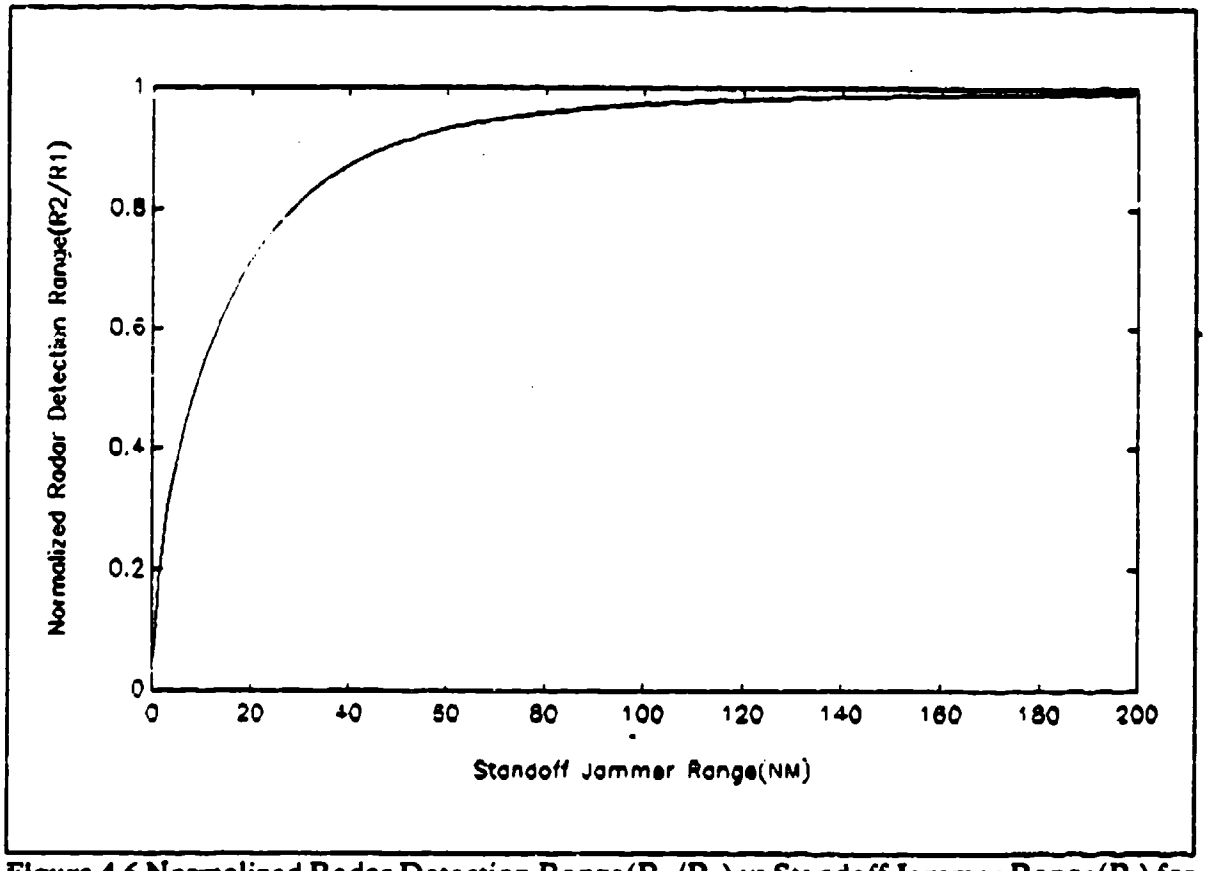

Figure 4.6 Normalized Radar Detection Range(R_2/R_1) vs Standoff Jammer Range(R_j) for the Sidelobe Barrage Jamming.

The normalized radar detection range is determined using Equation 4.21, 4.22 and 4.23. For the specific case of R_j = 50 NM the detection range R_2 under jamming is

$R_2 = 0.91 \times R_1$

$= 35.54$ NM (for $R_1 = 39.05$ NM)

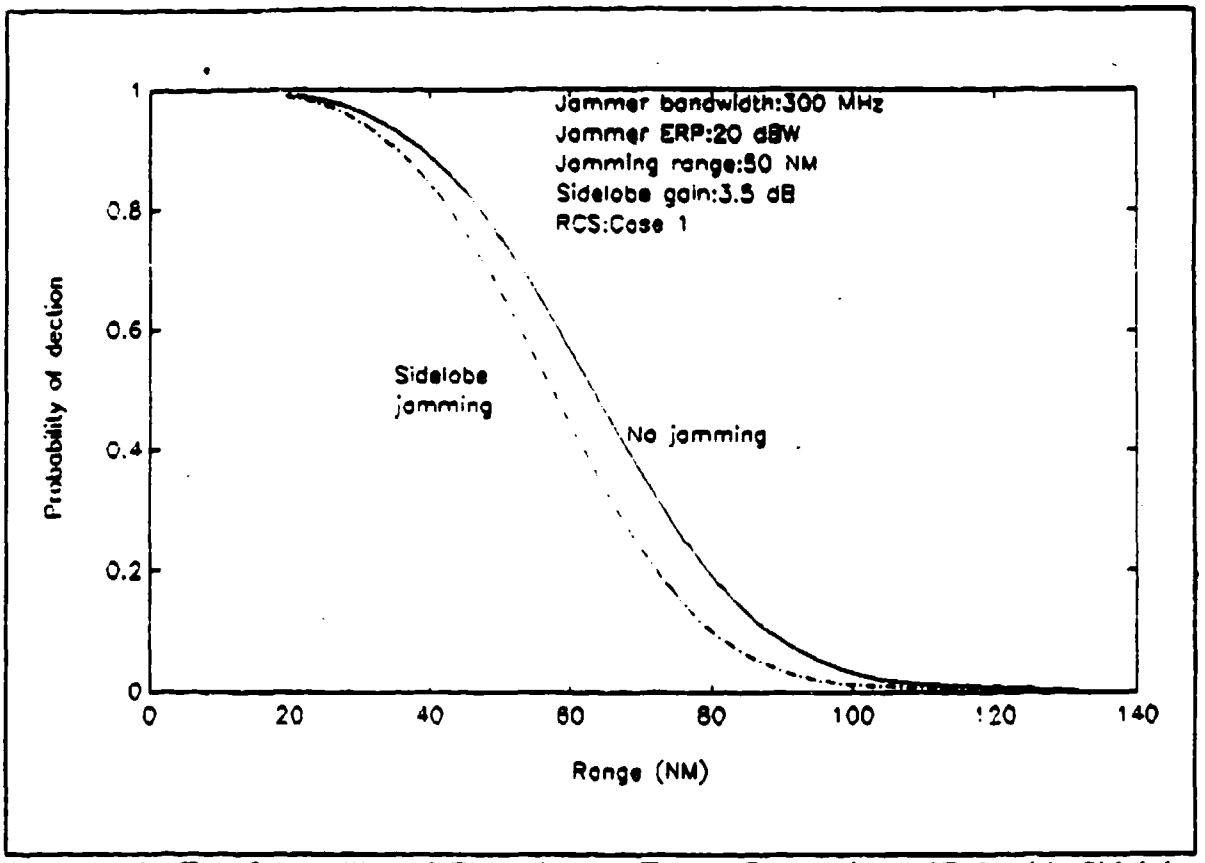

Figure 4.7 The Probability of Detection vs Target Range for ASR-9 with Sidelobe Barrage Jamming.

To determine detection range under jamming for all values of P_D for a radar to jammer range of 50 NM, use

$$R_2 = 0.91 \times \left(\frac{P_t G^2 \lambda^2 \sigma n E_i(n) PCR}{(4\pi)^3 \left(\frac{\log P_{FA}}{\log P_D} - 1\right) k T B F L}\right)^{\frac{1}{4}} \quad (4.24)$$

For given radar parameters, the results are plotted in Figure 4.7.

b. Maximum Detection Range with Spot Jamming

Next,let us consider sidelobe spot jamming with the jammer parameters of bandwidth of 10 MHz, jammer ERP of 25 dB, jamming range of 50 NM in the equation

$$\frac{J}{N} = \frac{P_j G_j G_{sl} \lambda^2}{(4\pi R_j)^2 L_j} \frac{1}{k T_o B_r F} \left(\frac{B_r}{B_j}\right) \quad (4.25)$$

The logarithmic form of the Equation 4.25 is as follows

$$(J/N)_{dB} = (ERP_j)_{dBW} + (G_{sl})_{dB} + 2(\lambda)_{dBm} - 2(R_j)_{dBm} + (B_r)_{Hz} - (B_j)_{Hz} - (L_j)_{dB} - (B_r)_{dB} - F + 181.99 \quad (4.26)$$

By substituting radar and jammer parameters in Equation 4.26

$$(J/N)_{dB} = 20 + 3.5 + 2(-9.85) - 2(10 \log(1852 * R_j)) - 70 - 5 + 181.993$$

$$= 110.79 - 20 \log(1852 * R_j) \quad (4.27)$$

Using Equations 4.27, 4.9 and 4.10, a graph of normalized radar detection range (R_2/R_1) vs jammer range(R_j) is plotted in Figure 4.8. This Figure shows a normalized detection range of 51 % for standoff jammer at 50 NM.

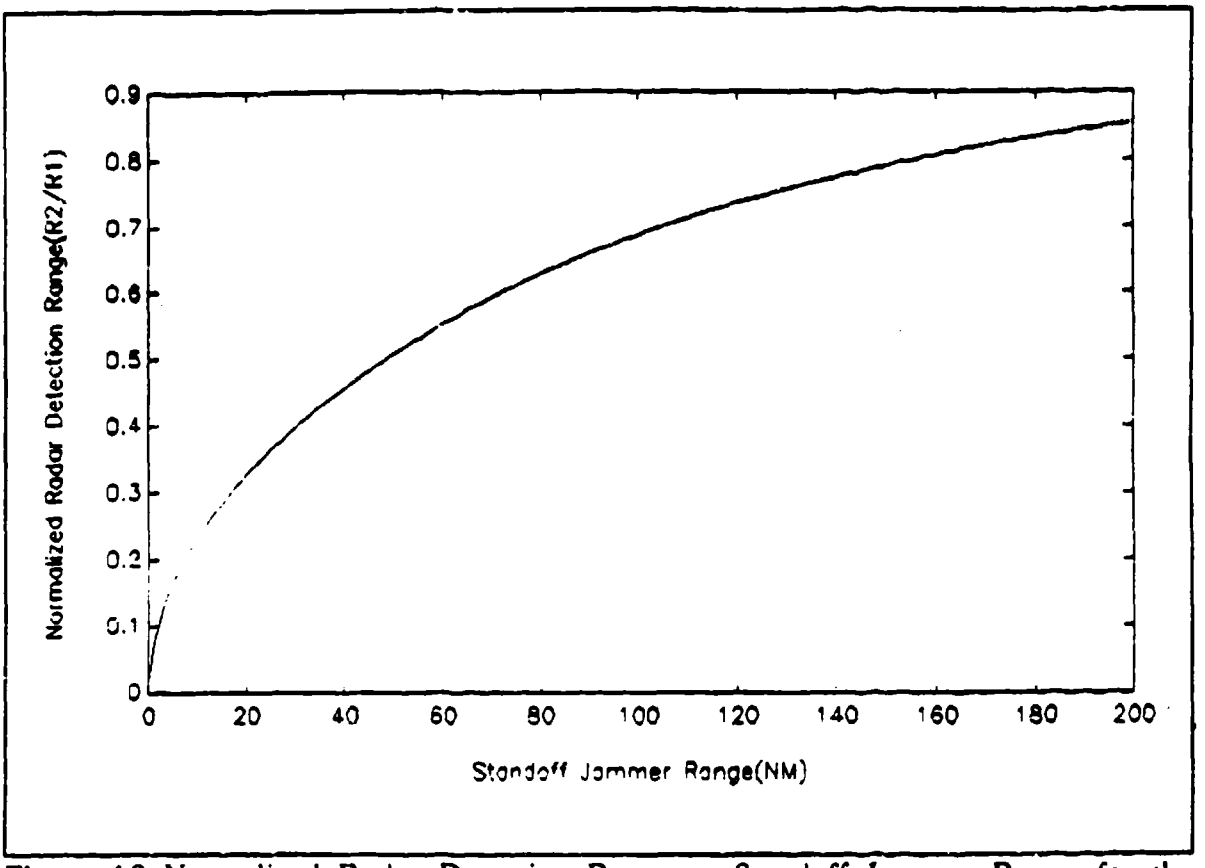

Figure 4.8 Normalized Radar Detection Range vs Standoff Jammer Range for the Sidelobe Spot Jamming.

For $P_D = 0.9$, $P_{FA} = 10^{-6}$ and $R_j = 50$NM, the detection range R_2 under sidelobe jamming is obtained as

$R_2 = 0.51 \times R_1$

$= 19.85$ NM

To determine detection range under jamming for any value of P_D

$$R_2 = 0.51 \times \left(\frac{P_t G^2 \lambda^2 \sigma n E_i(n) PCR}{(4\pi)^3 \left(\frac{\log P_{FA}}{\log P_D} - 1 \right) k T B F L} \right)^{\frac{1}{4}} \qquad (4.28)$$

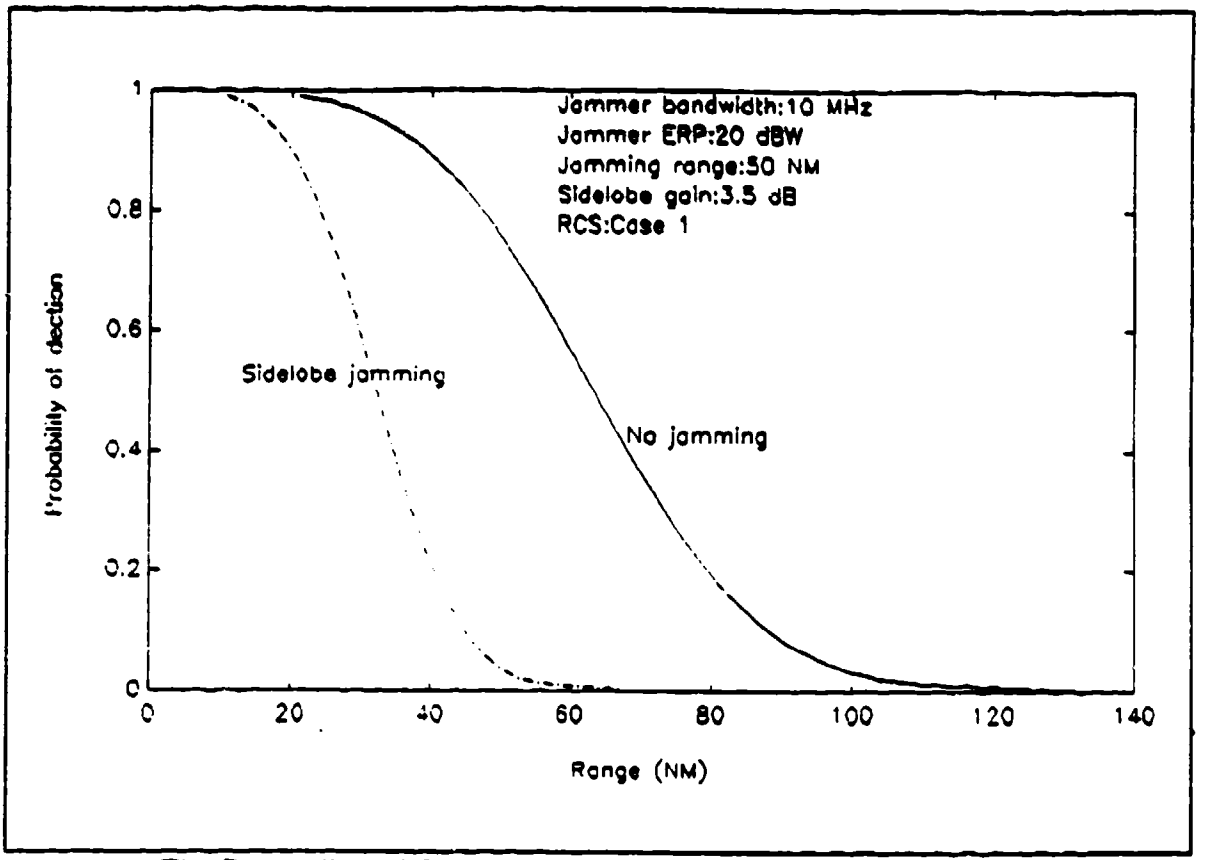

Figure 4.9 The Probability of Detection vs Target Range for ASR-9 with Sidelobe Spot Jamming.

For given radar parameters, the results are plotted in Figure 4.9.

c. *Burn-through Range and Crossover Range*

Using the appropriate J/S, crossover range and burn-through range for sidelobe jamming can be determined from the following equation

$$R = \left(\frac{P_t G_t}{P_j G_j} \frac{\sigma (R_j)^2}{4\pi} \frac{B_j}{B_r} \frac{PCR\, N_p}{K_j} \frac{L_j}{L_s} \frac{G_r}{G_{sl}} \left(\frac{J}{S}\right)\right)^{\frac{1}{4}} \qquad (4.29)$$

The above equation can be written in logarithmic form as follows

$$4R_B = (P_t)_{dBW} + (G_t)_{dB} - (ERP)_{dBW} + (\sigma)_{dBsm} + 2(R_j)_{dBm} - 10.992 + (B_j)_{Hz} - (B_r)_{Hz} + (PCR\ N_p)_{dB} - (K_j)_{dB} + (L_j)_{dB} - (L_s)_{dB} + (G_r)_{dB} - (G_{sl})_{dB} + (J/S)_{dB} \quad (4.30)$$

Substituting the relevant radar and jammer parameters(jammer bandwidth of 300 MHz and J/S = 1)

$(R_C)_{dB}$ = (60.79 + 33.5 - 20 + 2 x 49.67 - 10.99 + 24.99 + 13.2 - 12 + 30)/4 = 54.71 dB

which gives the crossover range for the sidelobe jamming case

R_C = 295,631 m = 159.6 NM

To compute burn-through range, a value of J/S for P_D of 0.5 is required. This was obtained as 0.045 earlier in this section. By substituting this value of J/S in logarithmic form in Equation 4.30 , a burn-through range(R_B) of 73 NM is found for the sidelobe jamming case.

Figure 4.10 shows the plot of signal and jamming power levels(both mainbeam and sidelobe) vs range. Signal power is computed from Equation 3.10. Mainbeam and sidelobe jamming powers are computed from Equations 3.11 and 3.14. It should be noted that both are at fixed range of 50 NM. Figure 4.10 can be used to determine crossover range and burn-through range for a specified J/S. For example, the burn-through range for mainbeam jamming for J/S of -10 dB is 16 NM from Figure 4.10.

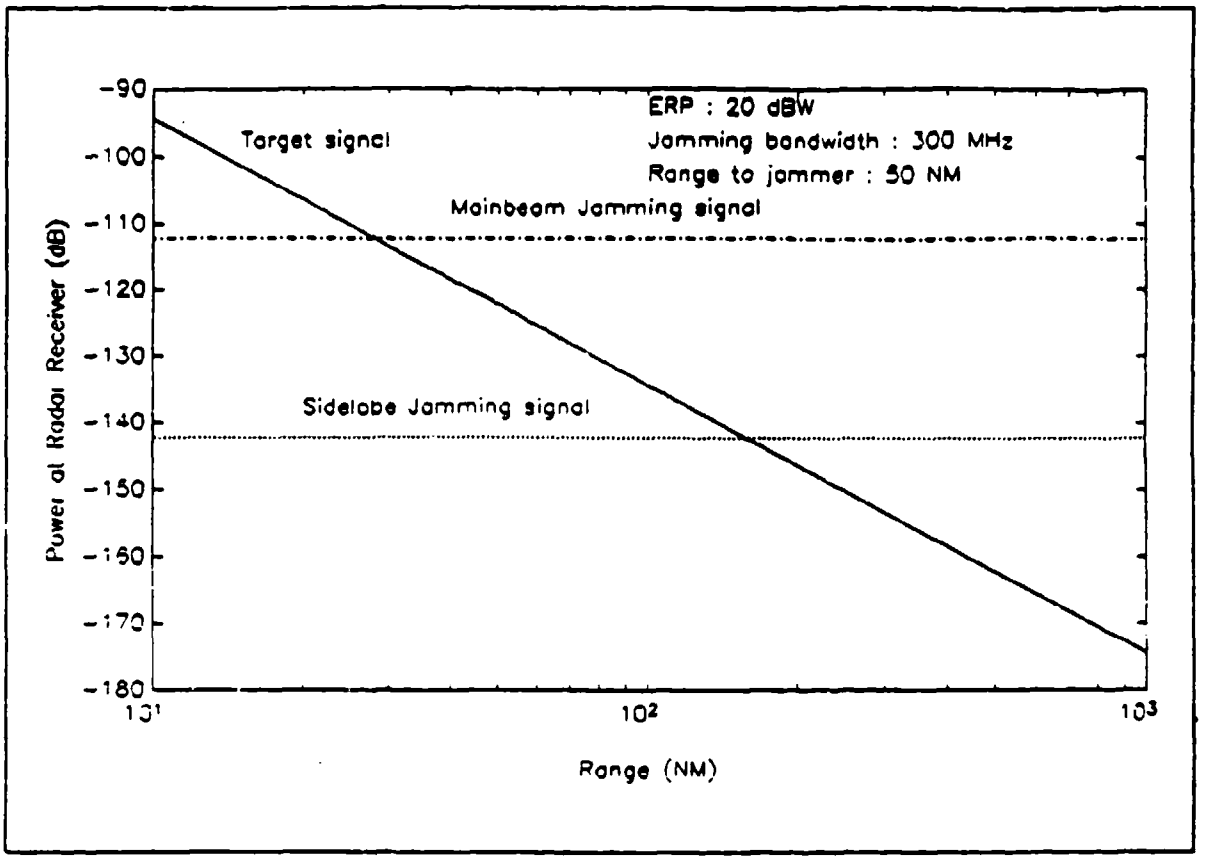

Figure 4.10 Burn-through Range of Mainbeam Jammer and Sidelobe Jammer.

V. ECCCM FEATURES

The primary goal of noise jamming of the ASR-9 is to prevent target detection and acquisition. ECCM techniques that can reduce the radar vulnerability to each type of jamming are summarized in the Table 5.1.

Jamming Type	Effects of jamming	ECCM Techniques
Mainbeam jamming		
* Barrage	Prevent target detection and acquisition	Jammer strobe processing Coherent integration
* Spot	Prevent target detection and acquisition, receiver saturation	Same as barrage jamming, plus frequency agility, wide dynamic range receivers
Sidelobe jamming		
* Barrage	Prevent target detection and acquisition	Low sidelobe antennas, sidelobe cancellation or blanking, coherent integration
* Spot	Prevent target detection and acquisition	Same as barrage noise(sidelobe),plus frequency agility

A. ECCM FOR MAINBEAM JAMMING

The noise jammer situation is basically an energy battle between the radar and the jammer. For mainbeam noise jamming, the advantage is with the jammer because the radar experiences a two way propagation loss of its energy as contrasted with the one way propagation loss between the radar and jammer. Thus, mainbeam jammers provide strong beacon like signals that betray their angular locations, which then can be exploited by the radar in weapon designation. If the radar is netted with other radars, the jamming target can be located through triangulation.

With mainbeam noise jamming, the radar design principles are clear.

1. **The radar must maximize the energy received from the target with respect to that received from the jammer**

It can maximize the received target energy by transmitting more average power, dwelling longer on the target, or increasing antenna gain. If the radar's data rate is fixed and a uniform angular search rate is dictated by mechanical or search strategy, then the only option for the radar is to increase its average transmitter power. The next option is to reduce the data rate requirement, thereby allowing a longer dwell time on the target.

2. **The second principle of ECCM design in mainbeam noise jamming is to minimize the amount of jamming energy accepted by the radar**

This is accomplished by spreading the transmitted frequency range of the radar over as wide a band as available while maintaining a radar bandwidth consistent with the radar range resolution requirement. For example, if a 150 to 300 MHz transmitting

frequency range is available at S band for a 1 MHz radar resolution bandwidth, then the potential for a 150 to 300 dilution of the jamming energy is possible. The ECCM objective is to force the jammer into a barrage jamming mode of operation. Operation of radars over a wider bandwidth than that dictated by range resolution requirements can be accomplished in several ways. Some radars incorporate a spectrum analyzer which provides an advance look at the interference environment. This allows the radar frequency to be tuned to that part of environment which contains minimum jamming energy. This can be defeated if the noise jammer has a look-through mode and can follow the radar frequency changes[Ref.4 p:222-223].

a. Frequency Agility

Frequency agility is the ability of the radar to transmit pulses of single frequency with a narrow bandwidth which can be changed from pulse to pulse. The purpose of this technique is to spread the jammer power over a wide band and thus dilute its spectral density. Frequency hopping by the radar is usually performed on a pulse to pulse basis for non-coherent modes and on a dwell to dwell basis when dwells are coherently processed. For an MTI radar, this period may be as short as every two transmitted pulses,and typically every three or four transmitted pulses. For pulsed Doppler radars, a block processing interval will consist of many pulses. Frequency agility forces a noise jammer into a barrage-jamming mode. Apart from ECCM benefit of frequency agility, it also reduces glint error, eliminates multiple time around echoes and decorrelates clutter.

b. Frequency Diversity

This is the ability to operate radars at a wide and diverse set of frequencies forcing the ECM system to provide a diversity equal to that used in the radar. Thus, frequency diversity uses several complementary radar transmissions at different frequencies, either from a single radar or several radars. The radar can operate in an integrated manner utilizing all the resources to the maximum extent. The diversity is usually limited by practical considerations to a finite number of frequencies(five to ten). Examples of this mode of operation are a 2-D surveillance radar coupled to a height-finder radar at a different frequency, or a number of spatially dispersed radars in a netted configuration at different frequencies.

c. Coherent Integration

Coherent integration narrows the receiving bandwidth and thus reduces the effectiveness of noise jamming.

3. **The third method which is employed to reduce the effect of mainbeam noise jamming is to narrow the antenna's beam**

This restricts the sector which is blanked by mainlobe noise jamming and also provides a strobe in the direction of the jammer. Strobes from two spatially separated radars pinpoint the jammer's location. However,with multiple jammer ghosting can be a problem.

B. ECCM FOR SIDELOBE JAMMING

The ECCM design principles for mainlobe noise jamming also apply to sidelobe noise jamming, with the exception that the sidelobe response in the direction of the jammer also

must be minimized. Barrage noise produced by a sidelobe jammer can deny detection and acquisition of a quiet target within the radar mainbeam, and can significantly degrade detection if directed at the radar sidelobe region. The following methods are used to reduce the vulnerability of radar to the sidelobe jamming.

1. Low Sidelobe Antennas

For those situations in which the jammer operates through the victim radar's receiving antenna sidelobes, reduction of the sidelobe gain will directly reduce the effectiveness of the jamming. A radar with only 20 dB sidelobes can easily be made useless over 360 degrees by a standoff noise jammer. Even its ability to obtain azimuth information on a jammer is impaired. Thus, low sidelobes are the first defense to combat standoff jamming[Ref.5 p:60]. Significant reduction of the sidelobe level can be achieved through the use of a suitably tapered illumination function across the receiving antenna aperture.

2. Sidelobe Blanker

The block diagram is given in Figure 5.1. The omnidirectional auxiliary antenna must have a gain of 3-4 dB above the sidelobes of the main antenna. When the signal in the auxiliary channel is more than the signal in the main channel then the signal must have entered through the sidelobe. In this case the gate is opened preventing the jamming signal from entering the receiver and display. Sidelobe blanker is effective only for low duty cycle pulse or swept frequency jamming. It should be noted that targets in the mainbeam are also discarded when blanking is done.

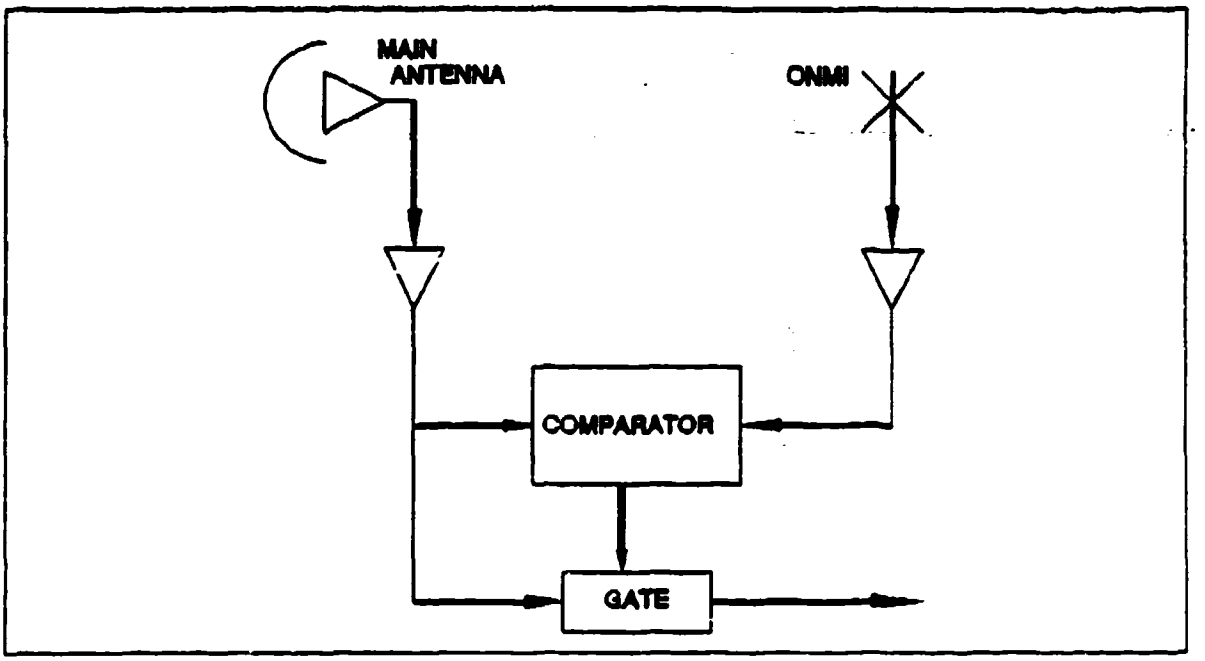

Figure 5.1 Sidelobe Blanker Block Diagram

3. Sidelobe Canceler

A coherent sidelobe canceler is a form of adaptive array antenna that uses a small number of elements to adaptively place nulls in the direction of jamming signal. This is a complex task and it requires at least one auxiliary antenna mainbeam loop for each jammer. A simplified block diagram is given in Figure 5.2. Present SLCs have the capability of reducing sidelobe noise jamming by 20 dB, but their theoretical performance is quoted much higher.

One of the limitations of the SLC is that the number of degrees of freedom is usually low, since only a small number of auxiliary antennas can be practically added to the main antenna. Because the maximum number of sidelobe jammers which can be handled is equal to the number of auxiliary antennas, the cancellation system is easily saturated. This problem is compounded by any jammer multipath from objects in the proximity of the radar

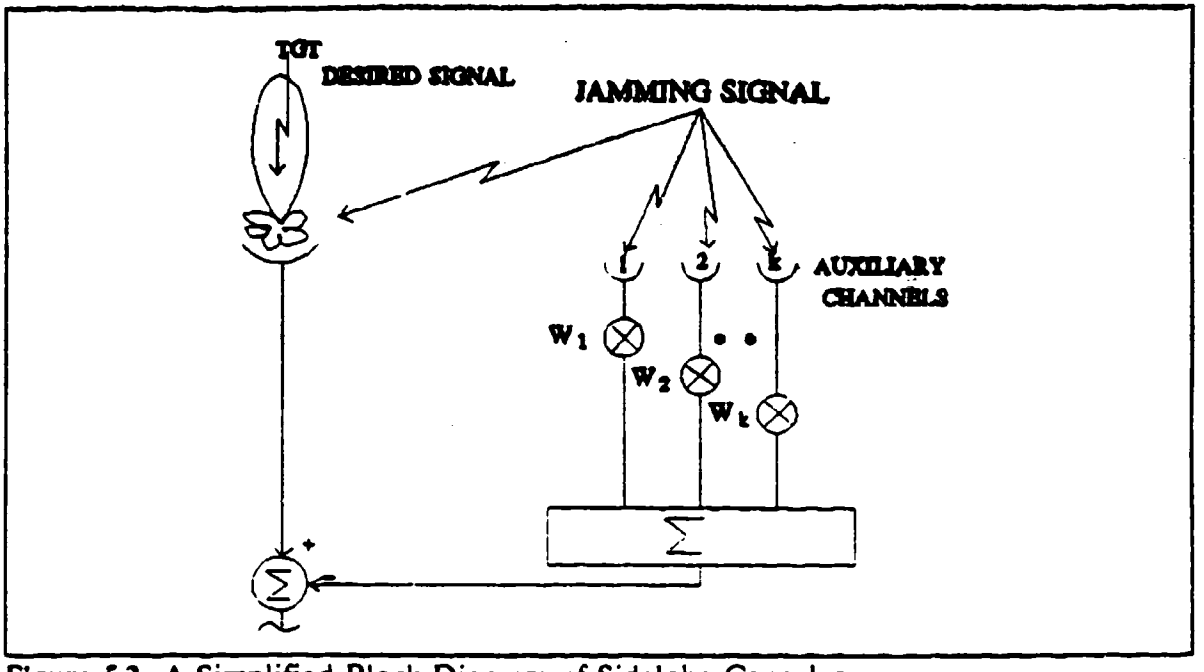

Figure 5.2 A Simplified Block Diagram of Sidelobe Canceler

which add an additional degree of freedom for each multipath signal having an angular direction significantly different than that of the main jammer. Another complication occurs for antennas whose cross polarization response is significantly different than its main polarization response. This causes two orthogonally polarized auxiliary antennas to be added for each degree of the SLC system.

VI. CONCLUSION AND RECOMMENDATION

This thesis describes the evaluation of radar performance degradation due to standoff jamming on surveillance radars. To keep the study unclassified, civilian radar ASR-9 was used as a victim radar. Jammer parameters representative of real life jammers were employed in the study. The maximum detection range of ASR-9 radar was evaluated for various cases. First of all P_D was determined as a function of target range without the use of jamming. Then P_D was determined as a function of target range with the standoff jamming. Both mainbeam and sidelobe jamming were considered. In each of the above two categories the performance degradation due to both barrage and spot jamming was determined.

As illustrated in chapter four, the barrage jamming through the radar antenna's mainbeam reduces the maximum detection range by factor of 78% of the normal detection range. Spot jamming through the mainbeam has 91% range reduction. Similarly, barrage jamming through the sidelobes has 9% range reduction and spot jamming through the sidelobes has 49 % range reduction of the normal maximum detection range. Thus, the mainbeam spot jamming is more effective as compared to the other jamming cases.

The Figure 6.1 show the maximum detection range under barrage jamming through the mainbeam, spot jamming through the mainbeam, barrage jamming through the sidelobes, spot jamming through the sidelobes and no jamming condition. For constant jammer ERP, mainbeam jamming is more effective than the sidelobe jamming and the spot jamming is more effective than the barrage jamming.

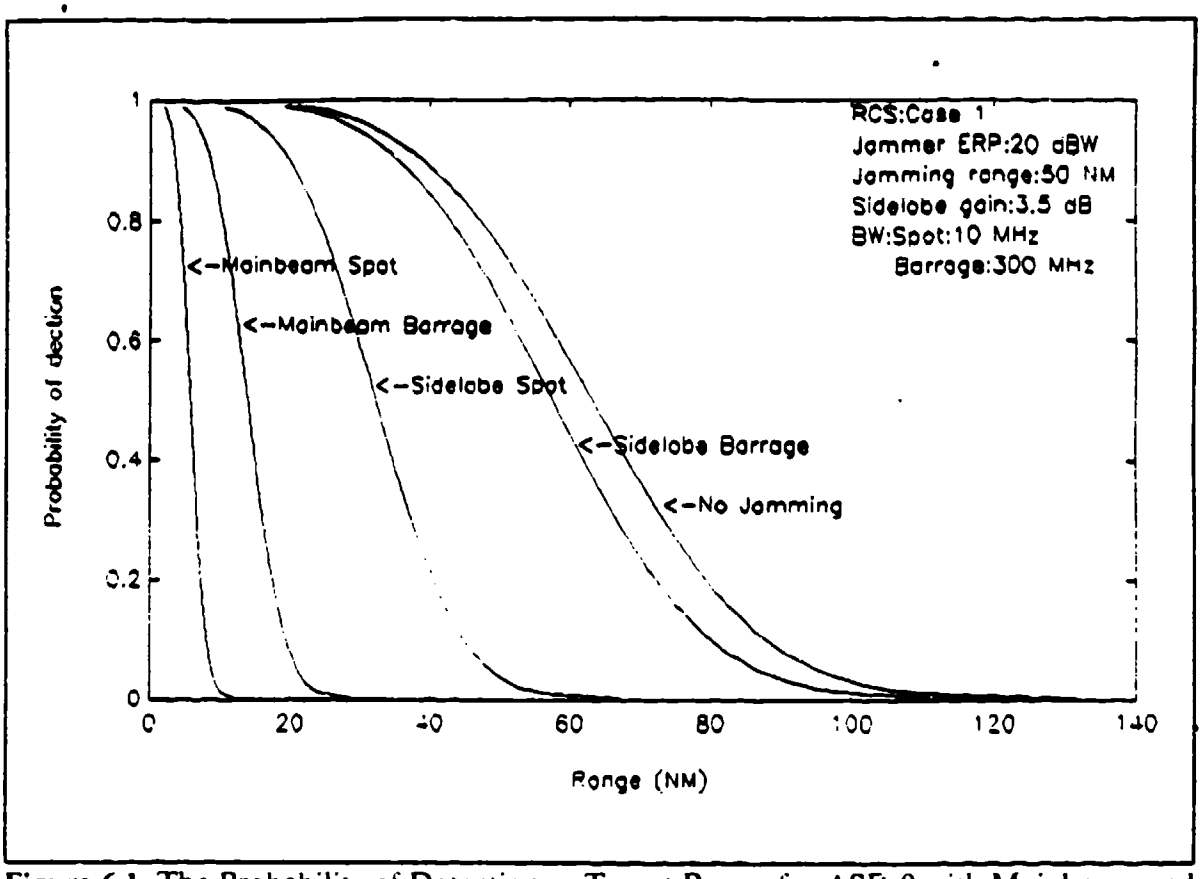

Figure 6.1 The Probability of Detection vs Target Range for ASR-9 with Mainbeam and Sidelobe jamming.

APPENDIX. A COMPUTER PROGRAMS

1. MATLAB PROGRAM FOR THE PROBABILITY OF DETECTION WITH/WITHOUT STANDOFF JAMMING

```
x=0.001:0.01:1;
b1=ones(100);
b2=b1(1,:);
b3=(log10(10^(-6))).*b2;
b4=10.*b2;
a1=b3./log10(x);
a2=10*log10(a1-1);
a3=(84.81-a2)/40;
a4=b4.^a3;
c1=0.092.*a4;
c2=0.22.*a4;
c3=0.91.*a4;
c4=0.51.*a4;
plot(c1,x,c3,x,a4,x,c4,x,c2,x)
xlabel('Range (NM)')
ylabel('Probability of dection ')
text(100,0.95,'RCS:Case 1')
text(100,0.9,'Jammer ERP:20 dBW')
text(100,.8,'Sidelobe gain:3.5 dB')
text(100,0.85,'Jamming range:50 NM')
text(100,0.75,'BW:Spot:10 MHz')
text(106,0.7,'Barrage:300 MHz')
text(5,0.7,'<-Mainbeam Spot ')
text(13,0.6,'<-Mainbeam Barrage')
text(32,0.5,'<-Sidelobe Spot')
text(61,0.4,'<-Sidelobe Barrage')
text(73,0.3,'<-No Jamming')
meta tfig61
```

2. MATLAB PROGRAM FOR BURN-THROUGH RANGE

```
x = 18520:1000:1852000;
a = 76.3277-40*log10(x);
b = -112.2974;
d = -142.2974;
c = x/1852;
for z = 1:1834;
 z1(z) = 1;
 b1 = z1;
end
b2 = b1(1,:);
c1 = b.*b2;
c2 = d.*b2;
semilogx(c,a,c,c1,'-.',c,c2,':');
xlabel('Range (NM)');ylabel('Power at Radar Receiver (dB)')
text(15,-100,'Target signal')
text(40,-110,'Mainbeam Jamming signal')
text(20,-140,'Sidelobe Jamming signal')
text(100,-95,'ERP : 20 dBW')
text(100,-100,'Jamming bandwidth : 300 MHz')
text(100,-105,'Range to jammer : 50 NM')
meta tfig410
```

APPENDIX. B PROBABILITY OF DETECTION VS TARGET RANGE

1. JAMMER ERP : 10 dBW (JAMMING RANGE : 50 NM)

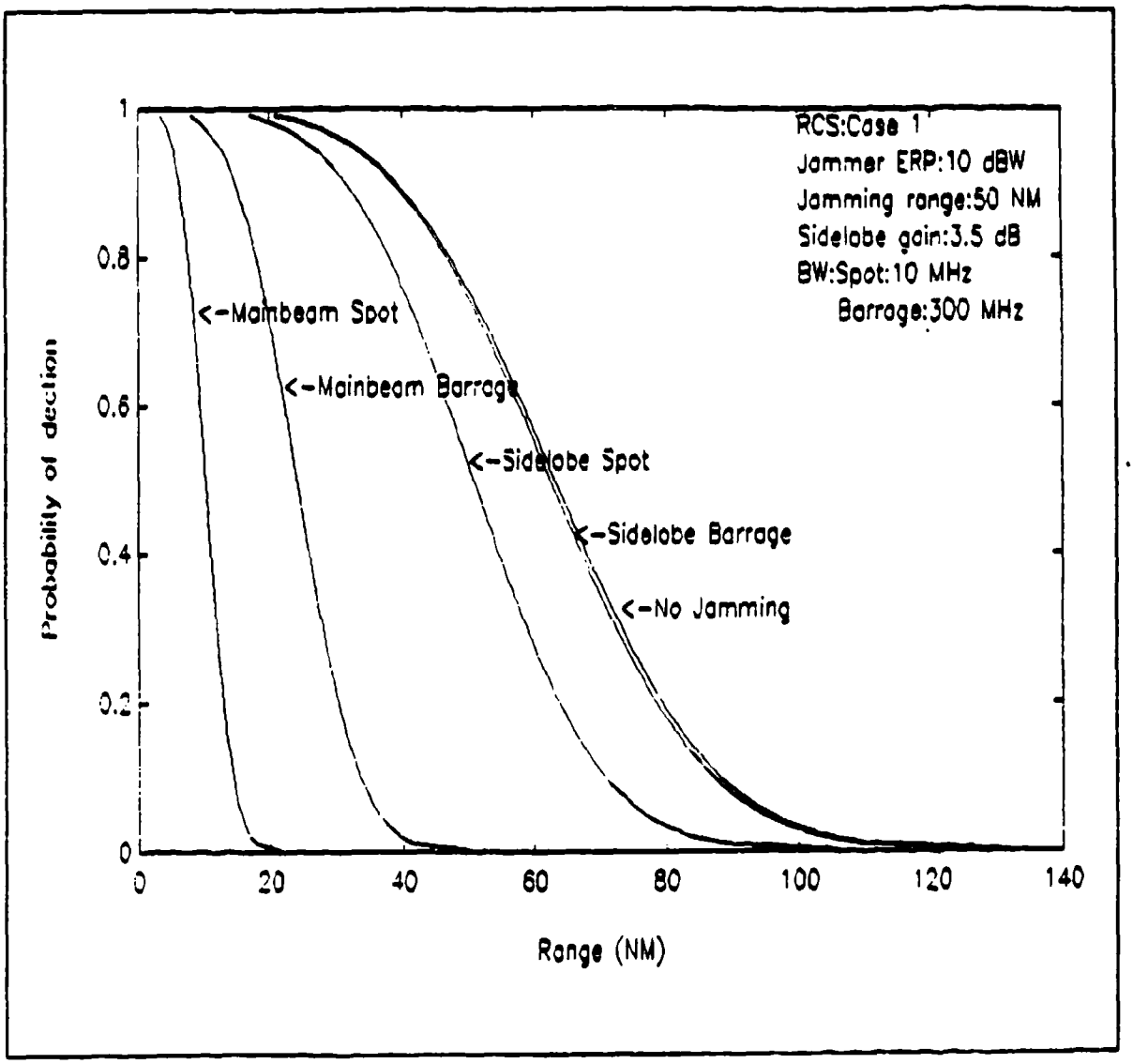

2. JAMMER ERP : 20 dBW (JAMMING RANGE : 50NM)

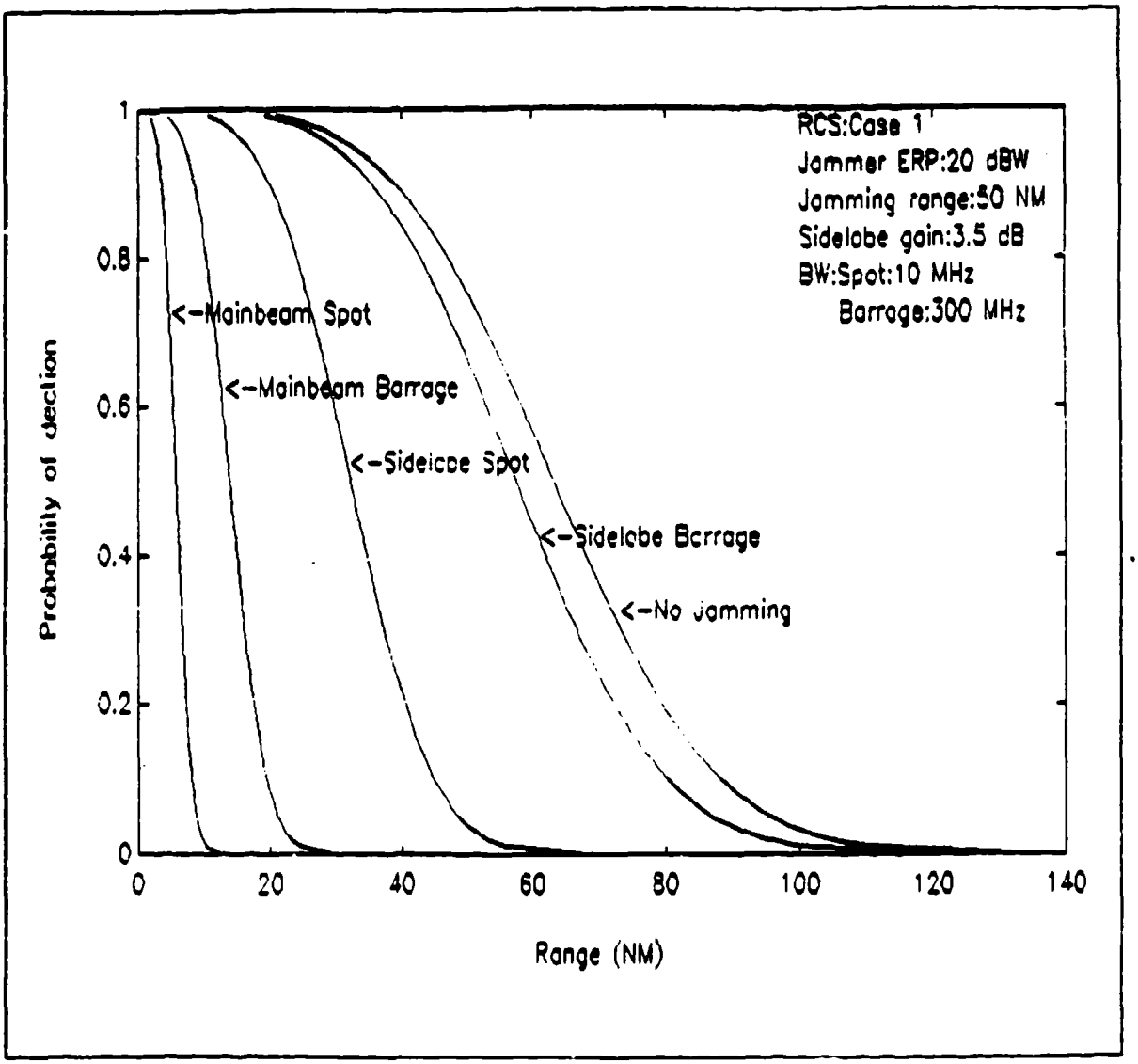

3. JAMMER ERP: 30 dBW (JAMMING RANGE : 50 NM)

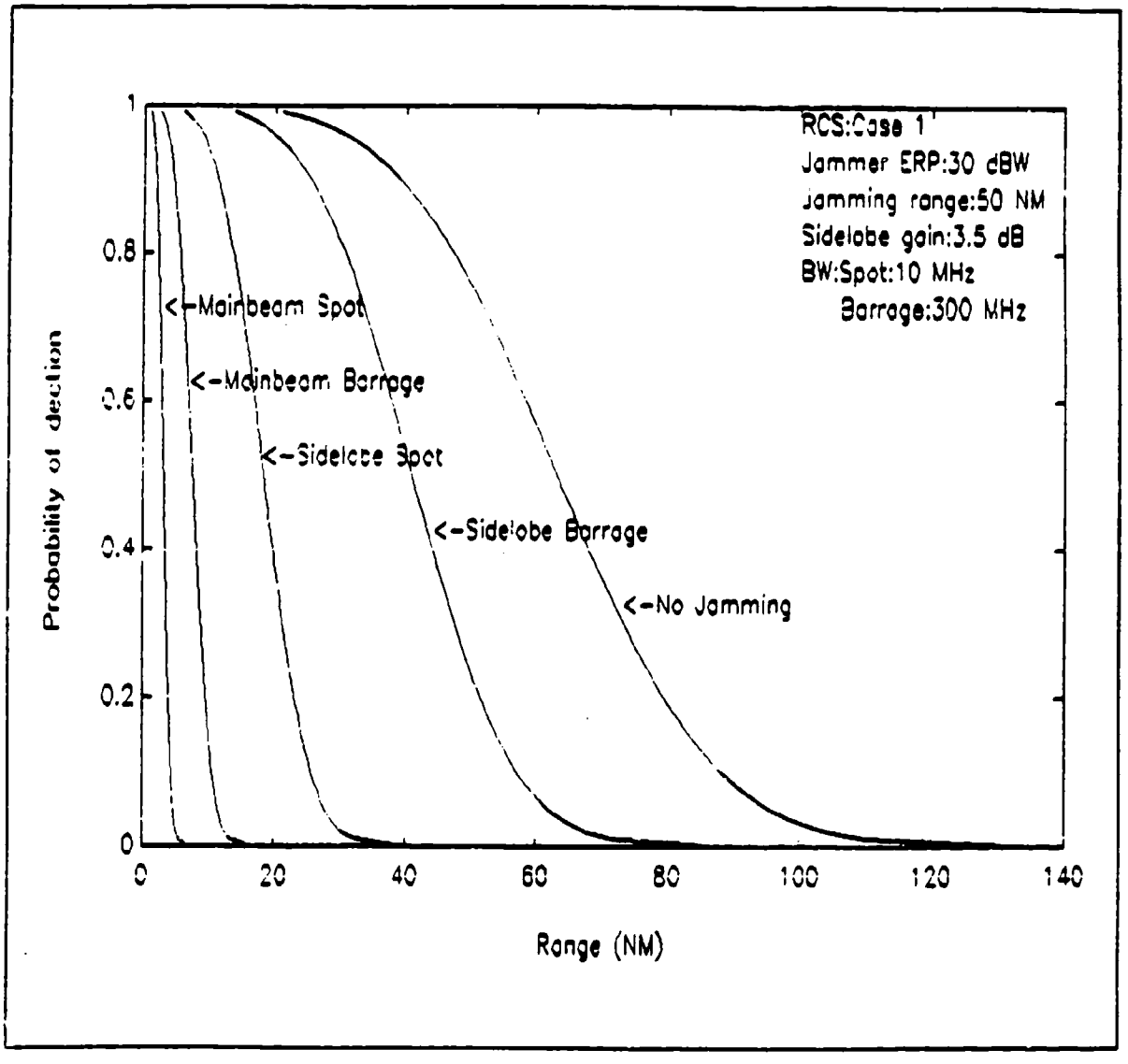

4. JAMMING RANGE 25 NM (JAMMER ERP : 20 dBW)

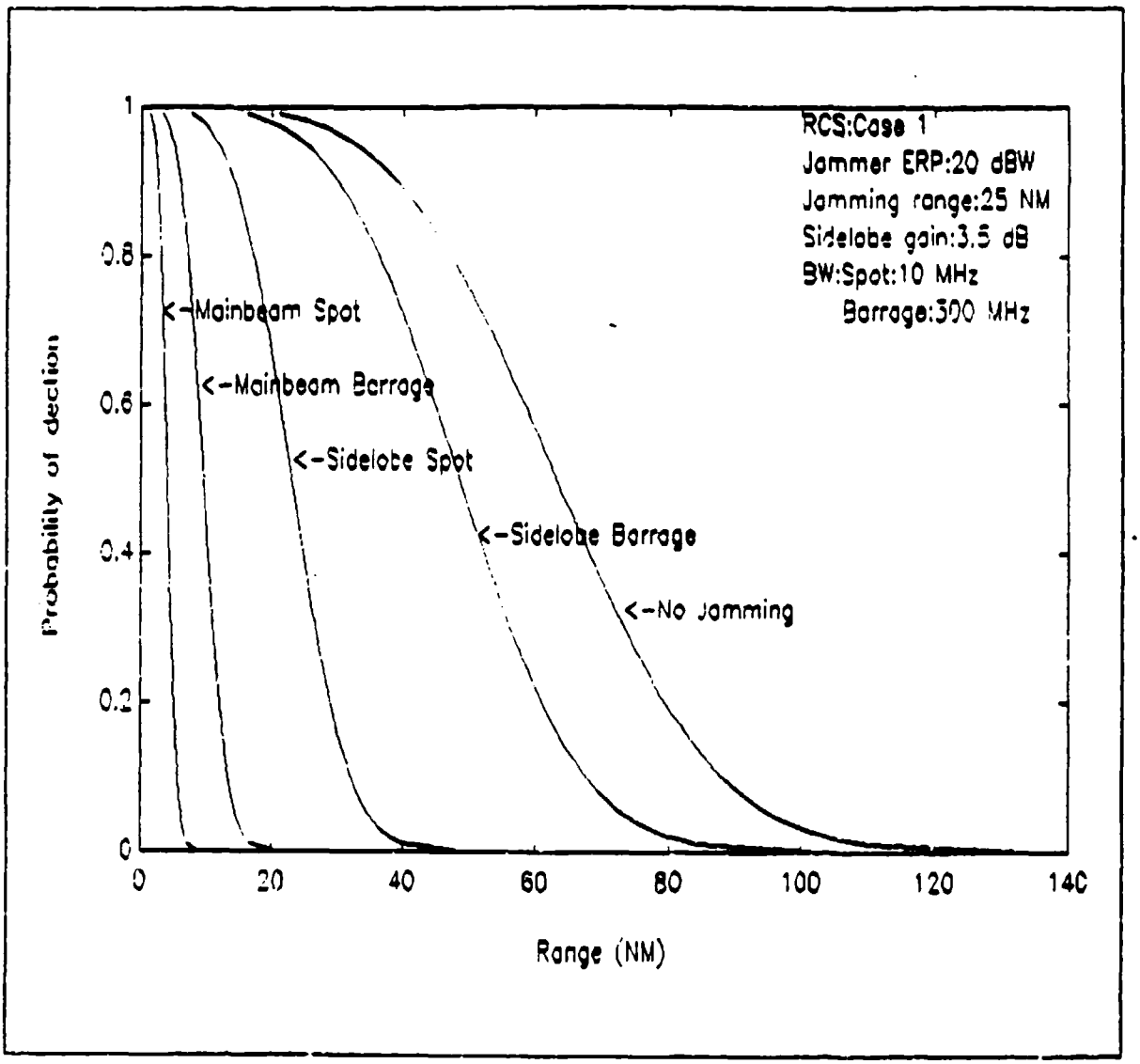

5. JAMMING RANGE 100 NM (JAMMER ERP : 20 dBW)

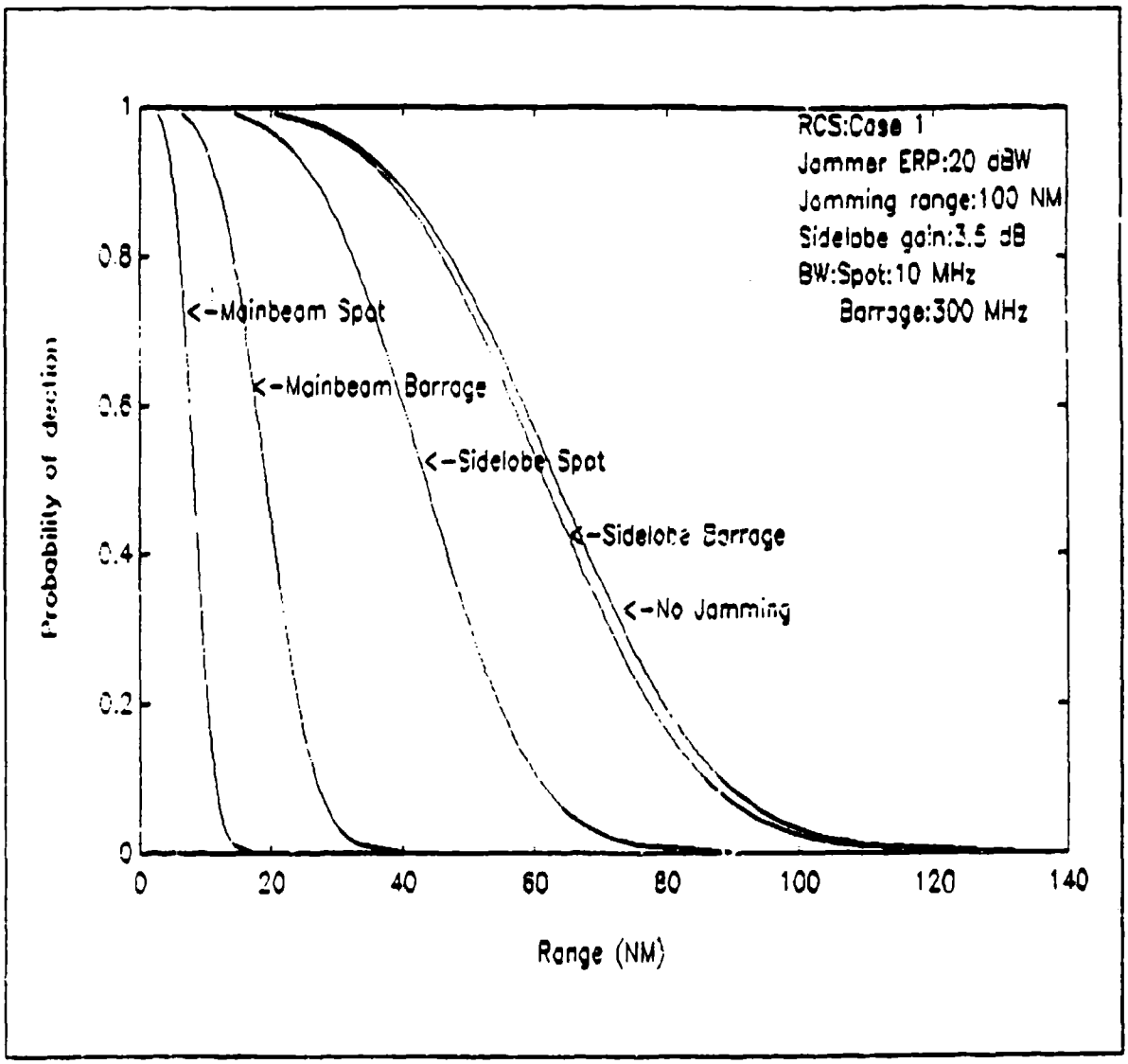

LIST OF REFERENCES

1. Skolnik,M.I., *Introduction to Radar Systems*, McGraw - Hill Pulishing Company, 1980.

2. Lothes,R.N., *Radar Vulnerability to Jamming*, Artech House, 1990.

3. Chrzanowski,E.J., *Active Radar Electronic Countermeasures*, Artech House,1990.

4. Schleher,D.C., *Introduction to Electronic Warfare*, Artech House Inc, 1986.

5. Peter R. Dax, *Noise Jamming of Long Range Search Radars*, Microwaves, September 1975

6. Barton,D.K., *Modern Radar System Analysis*, Artech House Inc, 1988.

7. Knott,E.F., *Radar Cross Section*, Artech House Inc, 1986.

8. Van Brunt,L.B., *Applied ECM Vol 1*, EW Engineering,Inc., 1987.

9. Van Brunt,L.B., *Applied ECM Vol 2*, EW Engineering,Inc., 1987.

10. *System Design Data For The ASR-9 (Final) in Response to Contract Article I ,Item 5b,* Westinghouse Electric Co, 1984.

11. *Advances in primary-Radar Technology*, The Licoln Laboratory Journal,Volume 2, Number 3,1989.

12. *Jane's airport equipment*. 1991-1992,Jane's Information Group.

13. Barton,D.K,Cook,C.F.,Paul Hamilton, Editors,*Radar Evaluation Handbook*, Artech House, 1991.

14. *The international countermeasurees handbook*,14th edition,1989.

INITIAL DISTRIBUTION LIST

	No.Copies
1. Defense Technical Information Center Cameron station Alexandria, VA 22304-6145	2
2. Library, Code 052 Naval Postgraduate School Monterey, CA 93943 -5002	2
3. Chairman, Code EW Department of Electrical Warfare Naval Postgraduate School Monterey, CA 93943	1
4. Professor G.S. Gill, Code EC/GL Department of Electrical and Computer Engineering Naval postgraduate School Monterey , CA 93943	2
5. Professor David Jenn, Code EC/JN Department of Electrical and Computer Engineering Naval Postgraduate School Monterey, CA 93943	1

6. Air Force Central Library(Air Force Collage) 2

Sindaebang Dong, Dong Jak Gu, Seoul

156-010, Republic of Korea

7. Library of Air force Academy 1

Sang Su Ri, Nam Yil Myon, Chongwon-Gun, Chungbook-Do

363-840, Republic of Korea

8. Chi, Yoon Kyu 2

150-26 Yong San Dong, Chung Ju city, Chung Chong Nam Do

380-090, Republic of Korea

9. Captain Kim Doo-Jong 1

SMC 1587 NPS

Monterey CA 93943

10. Devalla Raguhuram, Scientist 1

Defense Electronic Research LAB

Chandrayan Gutta

Hyderabad India 500005